

Entangled maximal mixings in $U_{\text{PMNS}} = U_\ell^\dagger U_\nu$, and a connection to complex mass textures

SVENJA NIEHAGE^a, WALTER WINTER^b

*Institut für Theoretische Physik und Astrophysik, Universität Würzburg,
D-97074 Würzburg, Germany*

Abstract

We discuss two different configurations of $U_{\text{PMNS}} = U_\ell^\dagger U_\nu$ with maximal mixings in *both* U_ℓ and U_ν . The non-maximal mixing angles are assumed to be small, which means that they can be expanded in. Since we are particularly interested in the implications for CP violation, we fully take into account complex phases. We demonstrate that one possibility leads to intrinsically large $\sin^2 2\theta_{13}$ and strong deviations from maximal mixings. The other possibility is generically close to tri-bimaximal mixing, and allows for large CP violation. We demonstrate how the determination of the θ_{23} octant and the precision measurement of δ_{CP} could discriminate among different qualitative cases. In order to constrain the unphysical and observable phases even further, we relate our configurations to complex mass matrix textures. In particular, we focus on phase patterns which could be generated by powers of a single complex quantity $\eta \simeq \theta_C \exp(i\Phi)$, which can be motivated by Froggatt-Nielsen-like models. For example, it turns out that in all of the discussed cases, one of the Majorana phases is proportional to Φ to leading order. In the entire study, we encounter three different classes of sum rules, which we systematically classify.

^aEmail: svenja.niehage@physik.uni-wuerzburg.de

^bEmail: winter@physik.uni-wuerzburg.de

1 Introduction

For Majorana neutrinos and the effective 3×3 -case, the neutrino mass matrix can be diagonalized by (here, we closely follow Refs. [1–3])

$$M_\nu^{\text{Maj}} = U_\nu M_\nu^{\text{diag}} U_\nu^T, \quad (1)$$

and the charged lepton mass matrix by

$$M_\ell = U_\ell M_\ell^{\text{diag}} U_\ell'^\dagger, \quad (2)$$

where U_ν , U_ℓ , and U_ℓ' are general unitary matrices. The (real) eigenvalues can be written as $M_\ell^{\text{diag}} = \text{diag}(m_e, m_\mu, m_\tau)$ and $M_\nu^{\text{diag}} = \text{diag}(m_1, m_2, m_3)$, and are, except from the absolute neutrino mass scale, experimentally known. The neutrino mixing matrix U_{PMNS} is generated as a product of two matrices U_ℓ and U_ν which enter the charged current interaction Lagrangian, *i.e.*, $U_{\text{PMNS}} = U_\ell^\dagger U_\nu$. Therefore, U_{PMNS} describes the relative rotation between the charged lepton U_ℓ and the neutrino mixing U_ν matrices, which turn the left-handed fields into the respective mass bases. Note that the mass matrix entries usually emerge as a product of the relevant Yukawa couplings and the vacuum expectation value of the Higgs. In addition, note that once the neutrino masses are known, the Majorana mass matrix M_ν^{Maj} can be reconstructed from U_ν according to Eq. (1). However, for the charged lepton mass matrix, an additional mixing matrix U_ℓ' turning the right-handed fields appears. Therefore, there is much more freedom involved in the reconstruction of M_ℓ , and we hence do not discuss specific structures for M_ℓ .

While the physical observables in U_{PMNS} are independent of the basis used for Eqs. (1) and (2), theoretical models often use the structure of the mass matrices as a starting point. These structures are often called “textures”. They are obviously basis dependent, and often predicted within a more general theoretical framework. For example, masses for quarks and leptons may arise from higher-dimension terms via the Froggatt-Nielsen mechanism [4] in combination with a flavor symmetry:

$$\mathcal{L}_{\text{eff}} \sim K_{ij} \langle H \rangle \eta^{n_{ij}} \bar{\Psi}_L^i \Psi_R^j + h.c.. \quad (3)$$

In this case, η is a small parameter $\eta = v/M_F$ which controls the flavor symmetry breaking. Here v are universal VEVs of SM (Standard Model) singlet scalar “flavons” that break the flavor symmetry, and M_F refers to the mass of super-heavy fermions, which are charged under the flavor symmetry. The SM fermions are given by the Ψ ’s, and K_{ij} are order unity (complex) numbers. The integer powers n_{ij} are solely determined by the quantum numbers of the fermions under the flavor symmetry (see, *e.g.*, Refs. [3, 5]), and the order one coefficients K_{ij} can be used to fit a particular texture to data. Obviously, the neutrino and charged lepton mass matrices in Eq. (1) and Eq. (2) are then, to a first approximation, described by the powers $M_{ij} \propto \eta_{ij}^n$, and U_ℓ or U_ν will, in general, *not* be diagonal. Therefore, large mixings may come from either the charged lepton or neutrino sector, as it has, for instance, been discussed in Refs. [6–12]. In this study, however, we discuss large mixing angles in *both* U_ℓ and U_ν , which lead to “entangled” maximal mixings (see also Ref. [13]). In addition, it is obvious from Eqs. (1) and (2) that if M_ν^{Maj} and M_ℓ are both real, then

U_{PMNS} will be real and there will be no leptonic CP violation. Therefore, we study the full complex case.

Entangled maximal mixings. In the first part of the study (*cf.*, Sec. 3), we use the standard parameterization for a CKM-like matrix

$$\widehat{U} = \begin{pmatrix} c_{12}c_{13} & s_{12}c_{13} & s_{13}e^{-i\widehat{\delta}} \\ -s_{12}c_{23} - c_{12}s_{23}s_{13}e^{i\widehat{\delta}} & c_{12}c_{23} - s_{12}s_{23}s_{13}e^{i\widehat{\delta}} & s_{23}c_{13} \\ s_{12}s_{23} - c_{12}c_{23}s_{13}e^{i\widehat{\delta}} & -c_{12}s_{23} - s_{12}c_{23}s_{13}e^{i\widehat{\delta}} & c_{23}c_{13} \end{pmatrix} \quad (4)$$

for both U_ℓ and U_ν , where $s_{ij} = \sin \widehat{\theta}_{ij}$ and $c_{ij} = \cos \widehat{\theta}_{ij}$. We adopt the purely phenomenological point of view that a number of mixing angles in U_ℓ and U_ν are maximal, and the others are small. The maximal mixing angles are assumed to be exactly maximal because they might be generated by a symmetry, and the small mixing angles are assumed to be $\mathcal{O}(\theta_C)$, which allows us to expand in them. We call a particular combination of maximal and small mixing angles a “configuration”. We study two of these configurations in Sec. 3, where the stars refer to the small mixing angles:

Configuration 1 with three max. mixing angles $(\theta_{12}^\ell, \theta_{13}^\ell, \theta_{23}^\ell, \theta_{12}^\nu, \theta_{13}^\nu, \theta_{23}^\nu) = (*, \frac{\pi}{4}, \frac{\pi}{4}, *, \frac{\pi}{4}, *)$

Configuration 2 with two max. mixing angles $(\theta_{12}^\ell, \theta_{13}^\ell, \theta_{23}^\ell, \theta_{12}^\nu, \theta_{13}^\nu, \theta_{23}^\nu) = (*, *, \frac{\pi}{4}, \frac{\pi}{4}, *, *)$

As we will demonstrate, both of these configurations lead to valid implementations of U_{PMNS} . We will use the currently allowed ranges for the observables to constrain the relationship between unphysical mixing angles and phases, and we will derive sum rules relating the observables.

Connection to quark sector and complex mass matrices. In order to establish a connection between the quark and lepton sectors, quark-lepton complementarity (QLC) [14–17] has been proposed as a possibility to account for the differences between the quark and lepton mixings. In QLC, the quark and lepton mixing angles are connected by QLC relations such as

$$\theta_{12} + \theta_C \simeq \pi/4. \quad (5)$$

Sum rules such as Eq. (5) do not only include observables from the lepton sector, but also the Cabibbo angle. They can be obtained if the mixing among the neutrinos and among the charged leptons is described by maximal or CKM-like mixing angles, such as in $U_{\text{PMNS}} \simeq V_{\text{CKM}}^\dagger U_{\text{bimax}}$ or similar constructions [1, 11, 18–23]. Instead of relying on special cases, extended quark-lepton complementarity (EQLC) [2] is based on the hypothesis that all mixing angles can only be from the set $\{\pi/4, \epsilon, \epsilon^2, \dots\}$ with $\epsilon \simeq \theta_C$.¹ Quite naturally, entangled maximal mixing configurations emerge from this assumption. In addition, it is a nice feature of EQLC to predict the textures of the charged lepton and neutrino mass matrices to be of the form $M_{ij} \sim \epsilon^{n_{ij}}$ with $n_{ij} \in \{0, 1, 2, \dots\}$, which allows for a direct connection to the Froggatt-Nielsen mechanism. Therefore, compared to many other approaches which focus on either the mixings or the hierarchies, EQLC aims to describe both the mixings and hierarchies. EQLC has successfully been applied to the see-saw mechanism [3], and

¹Other parameterizations of U_{PMNS} as a function of θ_C were, for instance, discussed in Refs. [24–28].

the effective 3×3 case has been extended to complex mass matrices [29]. For the seesaw case and real $\eta = \epsilon \simeq \theta_C$, a systematic connection to discrete flavor symmetries has been established in Ref. [30], and a connection to SU(5) GUTs was studied in Ref. [31]. The order of magnitude relations for the neutrino masses for M_ν^{diag} in Eq. (1) can in this context be written as

$$m_1 : m_2 : m_3 = \epsilon^2 : \epsilon : 1, \quad m_1 : m_2 : m_3 = 1 : 1 : \epsilon, \quad m_1 : m_2 : m_3 = 1 : 1 : 1, \quad (6)$$

where m_1, m_2 , and m_3 , denote the masses of the 1st, 2nd, and 3rd neutrino mass eigenstate. The 1st, 2nd, and 3rd equation in Eq. (6) describe a normal hierarchical (NH), inverse hierarchical (IH), and quasi degenerate (QD) spectrum, respectively.² We choose the NH case as an example for this study.

In the second part of this study (*cf.*, Sec. 4), we extend the texture concept of Refs. [2, 3, 29] to the complex case. Similar to Ref. [2], we parameterize the small mixing angles $\mathcal{O}(\epsilon)$ by powers of $\epsilon \simeq \theta_C$, *i.e.*, ϵ , ϵ^2 , and 0. Here we assume that higher powers than two in the neutrino sector are absorbed in the current measurement precision, and we approximate these by zero. We then define a texture by the leading orders in ϵ in the individual matrix entries, which are determined by the first non-vanishing coefficients. Compared to earlier works, we do not only use the absolute values of the leading order entries ϵ^n , but also their phases $n\Phi$ (except from a global phase, which can be removed for each matrix). This means that the leading order entry is given by $\eta^n = \epsilon^n \exp(in\Phi)$. For example, a texture may then read for the choice $\Phi = \pi/2$ as

$$M_\nu^{\text{Maj}} \sim \begin{pmatrix} \eta & \eta & \eta^2 \\ \eta & \eta & 0 \\ \eta^2 & 0 & 1 \end{pmatrix} = \begin{pmatrix} \epsilon e^{i\frac{\pi}{2}} & \epsilon e^{i\frac{\pi}{2}} & \epsilon^2 e^{i\pi} \\ \epsilon e^{i\frac{\pi}{2}} & \epsilon e^{i\frac{\pi}{2}} & 0 \\ \epsilon^2 e^{i\pi} & 0 & 1 \end{pmatrix}, \quad (7)$$

where a “0” corresponds to $\mathcal{O}(\epsilon^3)$ with an undefined phase. Note that in Froggatt-Nielsen-like (FN) models, one needs (at least) two standard model singlet flavon fields with different $U(1)_{\text{FN}}$ charges in order to produce CP violation, because for one fields the phase can be gauged away (see, *e.g.*, Refs. [32–34]). In this case, for patterns, such as in Eq. (7), it is required that one field dominate for mild hierarchies, such as the neutrino mass hierarchy. For example, one may have two different hierarchical VEVs, or two identical VEVs with very different $U(1)_{\text{FN}}$ charges. In these cases, the neutrino mass matrix will be dominated by one field, but the other field can be present in the charged lepton and quark mass matrices (or in the texture zeros; *cf.*, Eq. (7)). The phase Φ will then be the relative phase between the two VEVs of the fields. In addition, the order one coefficients are assumed to be real (and positive), *cf.*, Eq. (3). The advantage of a texture definition such as Eq. (7) is quite obvious: The condition to reproduce the correct powers of the phases in the texture leads to implications for the unphysical phases and the observables. In Sec. 4, we study this condition in combination with the configurations from Sec. 3, its effect on CP violation, and the emerging connection between the quark and lepton sectors via $\epsilon \simeq \theta_C$.

Before we present our analysis in Secs. 3 and 4, we summarize in Sec. 2 our notation and method. After our analysis, we summarize our results in Sec. 5.

²For NH neutrinos, one can compute ϵ from the current best-fit values, which gives $0.15 \lesssim \epsilon \lesssim 0.22$ (3σ).

2 Notation and method

In this section, we clarify our notation and describe some details of our method used in the following sections.

2.1 Sum rules

Throughout this study, we will encounter a number of different sum rules depending on the configuration studied and input used. In order to qualify as a sum rule, we require either a simple, testable connection among observables, which can be used to falsify our model (sum rule types I and II), or a simple relationship among observables and *one* unphysical quantity which allows for a straightforward extraction of this unphysical quantity (sum rule type III). In addition, we require that there be only bare angles in our sum rules, *i.e.*, that all trigonometric functions of the angles be expanded. For a systematic approach, we classify the sum rules according to the following scheme (with some examples from this study):

Type I sum rules (lepton sector sum rules) Sum rules relating lepton sector observables only; no unphysical quantities or model parameters are present in these sum rules. Example (*cf.*, Sec. 3.2.1):

$$\theta_{23} + \frac{1}{2} \theta_{13}^2 \simeq \frac{\pi}{4}.$$

This type of sum rules can be used to falsify our model if *all* of the contributing observables (at least two) are measured. It can be analogously translated in to the quark sector.

Type II sum rules (QLC-type sum rules) Sum rules relating lepton and quark sector observables; no unphysical quantities or model parameters are present in these sum rules (see, *e.g.*, Refs. [17, 30, 35]). Example (*cf.*, Table 5):

$$\theta_{23} - \frac{1}{4} \theta_C^2 \simeq \frac{\pi}{4}.$$

This type of sum rules can be used to falsify our model if *all* of the contributing observables (at least one from the lepton sector) are measured

Type III sum rules (observable-model sum rules) Sum rules relating observables from one or both sectors to unphysical quantities or model parameters. We distinguish two types:

Type IIIa sum rules relate observables to unphysical parameters, such as the mixing angles or phases in U_ℓ or U_ν (see, *e.g.*, Refs. [13, 20]). Example (*cf.*, Table 5):

$$\theta_{12} + \frac{1}{\sqrt{2}} \cos \delta^\ell \theta_C \simeq \frac{\pi}{4}.$$

Type IIIb sum rules relate observables to model parameters, such as the phase Φ introduced just before Eq. (7). Example (*cf.*, Table 5):

$$\sin \delta_{\text{CP}} \simeq \sqrt{2} \theta_C \sin 2\Phi.$$

These sum rules can be used to obtain (model-dependent) information on the unphysical quantities or model parameters if *all* of the contributing observables (at least one from the lepton sector) are measured.

2.2 Parameterization of the mixing matrices

Let us now give some details on the parameterization of our mixing matrices. A general unitary 3×3 matrix U_{unitary} can be written as

$$U_{\text{unitary}} = \Gamma \cdot \text{diag}(1, e^{i\hat{\varphi}_1}, e^{i\hat{\varphi}_2}) \cdot \hat{U} \cdot \text{diag}(e^{i\hat{\alpha}_1}, e^{i\hat{\alpha}_2}, 1) = \Gamma \cdot D \cdot \hat{U} \cdot K, \quad (8)$$

where the phases $\hat{\varphi}_1$, $\hat{\varphi}_2$, $\hat{\alpha}_1$, and $\hat{\alpha}_2$, take their values in the interval $[0, 2\pi]$, Γ is a global phase factor, and \hat{U} is the (CKM-like) standard parameterization in Eq. (4). We then obtain the PMNS mixing matrix from the charged current interaction Lagrangian as

$$U_{\text{PMNS}} = U_\ell^\dagger U_\nu = K_\ell^\dagger \hat{U}_\ell^\dagger D_\ell^\dagger D_\nu \hat{U}_\nu K_\nu = \hat{U}_\ell^\dagger D \hat{U}_\nu K_\nu. \quad (9)$$

Note that we have already ignored an unphysical overall phase in U_{PMNS} . Furthermore, as the last step, we have rotated away K_ℓ by re-phasing the charged lepton fields, and we have defined $D = D_\ell^\dagger D_\nu$. We define the remaining phases by $D = \text{diag}(1, e^{i\varphi_1}, e^{i\varphi_2})$ and $K_\nu = \text{diag}(e^{i\alpha_1}, e^{i\alpha_2}, 1)$. The effect of the phases in D has, for example, been discussed in Ref. [13]. The PMNS matrix in Eq. (9) can, physics-wise equivalently, be directly written as

$$U_{\text{PMNS}} = U_\ell^\dagger U_\nu = \hat{U} \cdot \text{diag}(e^{i\phi_1}, e^{i\phi_2}, 1), \quad (10)$$

where \hat{U} is a CKM-like matrix that is on the form as in Eq. (4), and the phases ϕ_1 and ϕ_2 are the Majorana phases. The CKM-like matrix \hat{U} in Eq. (10) is described by the solar angle θ_{12} , the reactor angle θ_{13} , the atmospheric angle θ_{23} , and one Dirac CP-phase δ , which we identify in the standard parameterization of Eq. (4) by using $\hat{\theta}_{ij} \rightarrow \theta_{ij}$ and $\hat{\delta} \rightarrow \delta$. Note that we have used $U_\ell = \hat{U}_\ell$, and that we will use $U'_\ell = D'_\ell \hat{U}'_\ell K'_\ell = \hat{U}'_\ell K'_\ell$ in Eq. (2), *i.e.*, in all cases, $D_\ell = 1$, $K_\ell = 1$, and $D'_\ell = 1$. Consequently, $D = D_\nu$ in Eq. (9).³ With these restrictions, the set of parameters

$$(\theta_{12}^\ell, \theta_{13}^\ell, \theta_{23}^\ell, \delta^\ell, \theta_{12}^\nu, \theta_{13}^\nu, \theta_{23}^\nu, \delta^\nu, \varphi_1, \varphi_2, \alpha_1, \alpha_2) \quad (11)$$

fully determines Eqs. (1) and (9). For our configurations, we will later on fix some of the θ_{ij} 's to $\pi/4$, and assume the other θ_{ij} 's to be small. For the phases, we initially do not make

³This restriction neither affects Eq. (9) and its fit to data, nor constrains the effective neutrino mass matrix Eq. (1). In addition, the constraint $K_\ell = 1$ does not change Eq. (2) because it only appears as a product with K'_ℓ . However, the choices $D_\ell = D'_\ell = 1$, which are multiplied to Eq. (2) from the outside, limit the set of allowed phases in M_ℓ . One should keep this additional degree of freedom in mind when one interprets our examples for possible M_ℓ .

any special assumptions. If one is interested in the specific form of the charged lepton mass matrix Eq. (2), one needs to specify the set of parameters

$$(\theta_{12}^{\ell'}, \theta_{13}^{\ell'}, \theta_{23}^{\ell'}, \delta^{\ell'}, \alpha_1^{\ell'}, \alpha_2^{\ell'}) \quad (12)$$

as well.

2.3 Calculation of observables by re-phasing invariants

As soon as U_{PMNS} is computed from a set of parameters Eq. (11) used in Eq. (9), one can extract the physical observables by using re-phasing invariants (see, *e.g.*, Ref. [36]). We choose the three quadratic re-phasing invariants $|U_{13}|^2$, $|U_{23}|^2$ and $|U_{12}|^2$ to determine the three angles θ_{13} , θ_{23} and θ_{12} as follows:

$$\sin^2 \theta_{13} = |U_{13}|^2 \quad (13)$$

$$\sin^2 \theta_{23} = \frac{|U_{23}|^2}{1 - |U_{13}|^2} \quad (14)$$

$$\sin^2 \theta_{12} = \frac{|U_{12}|^2}{1 - |U_{13}|^2}. \quad (15)$$

The observable phases δ_{CP} and the two Majorana phases ϕ_1 and ϕ_2 are determined with the quadratic invariant $|U_{22}|^2$ and these CP-odd quartic invariants: the Jarlskog invariant $J = \text{Im}(U_{22}U_{11}U_{21}^*U_{12}^*)$ [37], $(U_{13}U_{11}^*)^2$, and $(U_{13}U_{12}^*)^2$. The two following equations determine δ_{CP} and its sign:

$$\begin{aligned} J &= c_{12}c_{23}c_{13}^2 s_{23}s_{13}s_{12} \sin \delta_{\text{CP}}, \\ |U_{22}|^2 &= c_{12}^2 c_{23}^2 + s_{12}^2 s_{23}^2 s_{13}^2 - c_{12}c_{23}s_{12}s_{23}s_{13}2 \cos \delta_{\text{CP}}. \end{aligned} \quad (16)$$

Since in our definition of the Majorana phases (in Eq. (10)) physical quantities depend only on $2\phi_1$ and $2\phi_2$, we only determine their double values as

$$\begin{aligned} 2\phi_1 &= -\arg((U_{13}U_{11}^*)^2) - 2\delta_{\text{CP}}, \\ 2\phi_2 &= -\arg((U_{13}U_{12}^*)^2) - 2\delta_{\text{CP}}. \end{aligned} \quad (17)$$

2.4 Consistency check with data

As the last step, we will compare the extracted observables to data in order to check potential constraints on the unphysical quantities. Whenever we make quantitative estimates, we will use the following numbers [38]:

$$\begin{aligned} \sin^2 \theta_{13} &\lesssim 0.04 \quad (3\sigma), \\ \sin^2 \theta_{12} &= 0.3 \pm 9\% \quad (1\sigma), \quad 0.24 \lesssim \sin^2 \theta_{12} \lesssim 0.40 \quad (3\sigma), \\ \sin^2 \theta_{23} &= 0.5 \pm 16\% \quad (1\sigma), \quad 0.34 \lesssim \sin^2 \theta_{23} \lesssim 0.68 \quad (3\sigma). \end{aligned} \quad (18)$$

We choose the 3σ allowed ranges, unless explicitly mentioned otherwise.

3 Entangled maximal mixing configurations

In this section, we discuss two different configurations with maximal mixing angles in both U_ℓ and U_ν , where the stars denote small mixing angles $\mathcal{O}(\theta_C)$:

1. Three maximal mixing angles: $(\theta_{12}^\ell, \theta_{13}^\ell, \theta_{23}^\ell, \theta_{12}^\nu, \theta_{13}^\nu, \theta_{23}^\nu) = (*, \frac{\pi}{4}, \frac{\pi}{4}, *, \frac{\pi}{4}, *)$
2. Two maximal mixing angles: $(\theta_{12}^\ell, \theta_{13}^\ell, \theta_{23}^\ell, \theta_{12}^\nu, \theta_{13}^\nu, \theta_{23}^\nu) = (*, *, \frac{\pi}{4}, \frac{\pi}{4}, *, *)$

Since the small mixing angles are $\mathcal{O}(\theta_C)$, we can use them for expansions. Note that these configurations are not the only ones leading to a valid U_{PMNS} . We show a list of possible configurations in App. A, where we also describe the selection criteria for the ones discussed analytically here. Out of the 44 configurations found, 38 have entangled maximal mixings. Therefore, the cases discussed in this study might be rather typical than the remaining six configurations with maximal mixings in either U_ℓ or U_ν only.

As described in Sec. 2, we compute the observables using invariants, and we discuss the effects from the current bounds. Where applicable, we will discuss different implementations for the small mixing angles. Note that, at this point, we do not assume specific values for the small mixing angles, such as powers of θ_C . Therefore, there will not be any connection to the quark sector yet. However, our conclusions will be less model-dependent than the ones from the following section.

3.1 Three maximal mixing angles: $(\theta_{12}^\ell, \theta_{13}^\ell, \theta_{23}^\ell, \theta_{12}^\nu, \theta_{13}^\nu, \theta_{23}^\nu) = (*, \frac{\pi}{4}, \frac{\pi}{4}, *, \frac{\pi}{4}, *)$

This configuration is given by three maximal mixing angles, one in the neutrino sector, θ_{13}^ν , and two in the charged lepton sector, θ_{13}^ℓ and θ_{23}^ℓ . Note again that the other mixings angles θ_{12}^ℓ , θ_{12}^ν , and θ_{23}^ν are assumed to be small, *i.e.*, $\mathcal{O}(\theta_C)$, which means that we can use them for expansions. For the sake of simplicity, it is convenient to use some phase re-definitions for this configuration:

$$\chi \equiv \delta^\ell - \varphi_1, \quad \beta \equiv \delta^\ell - \delta^\nu - \varphi_2, \quad \gamma \equiv \varphi_1 - \varphi_2. \quad (19)$$

With these re-definitions, we expand $\sin^2 \theta_{13}$ to first order as⁴

$$\begin{aligned} \sin^2 \theta_{13} = & \frac{3}{8} - \frac{\sqrt{2}}{4} \cos \beta + \theta_{12}^\ell \left(\frac{1}{2} \cos(\delta^\ell - \beta) - \frac{\sqrt{2}}{4} \cos \delta^\ell \right) + \\ & + \theta_{23}^\nu \left(\frac{1}{4} \cos \gamma - \frac{\sqrt{2}}{4} \cos(\gamma - \beta) \right) + \mathcal{O}(\theta_k^2). \end{aligned} \quad (20)$$

Here the symbol θ_k^2 stands for all small mixing angles and combinations thereof, such as $\theta_{12}^\ell \theta_{23}^\nu$ and $(\theta_{23}^\nu)^2$. Obviously, the *zeroth* order term in this expansion is given by $3/8 -$

⁴In the following, we will expand the observables to the minimum order for which we recover the main qualitative features. For example, if the *zeroth* order vanishes, or the terms from different orders are numerically comparable, we will include higher orders.

$\sqrt{2}\cos\beta/4$, which means that $\sin^2\theta_{13}$ is expected to be large. From Eq. (18), however, we know that $\sin^2\theta_{13} \lesssim 0.04$, which leads to $\cos\beta \gtrsim 0.95$ to *zeroth* order.

The atmospheric mixing angle is given by

$$\begin{aligned} \sin^2\theta_{23} = & \frac{2}{5 + 2\sqrt{2}\cos\beta} \\ & + \frac{2}{(5 + 2\sqrt{2}\cos\beta)^2} \theta_{12}^\ell \left(-4\cos(\delta^\ell - \beta) + \sqrt{2}\cos\delta^\ell + 2\cos(\delta^\ell + \beta) - 2\sqrt{2}\cos(2\beta - \delta^\ell) \right) - \\ & - \frac{4}{(5 + 2\sqrt{2}\cos\beta)^2} \theta_{23}^\nu \left(4\cos\gamma + 2\sqrt{2}\cos(\gamma - \beta) + \sqrt{2}\cos(\beta + \gamma) \right) + \mathcal{O}(\theta_k^2). \end{aligned} \quad (21)$$

This implies that to *zeroth* order, we have $\sin^2\theta_{23} = 2/(5 + 2\sqrt{2}\cos\beta)$. Since we have a lower bound for $\cos\beta$ from the $\sin^2\theta_{13}$ upper bound, $\sin^2\theta_{23}$ must be smaller than maximal mixing. From the *zeroth* order constraint on $\cos\beta$, we obtain $\sin^2\theta_{23} \lesssim 0.26$ to *zeroth* order, which is below the allowed range for $\sin^2\theta_{23}$ in Eq. (18). Therefore, one has to include higher order corrections such that $\sin^2\theta_{23}$ is shifted up into the allowed range. Nevertheless, it will stay on the lower edge of the allowed range, which makes this configuration easily testable in future experiments.

As the third observable, the solar mixing angle is determined by

$$\begin{aligned} \sin^2\theta_{12} = & \frac{2}{5 + 2\sqrt{2}\cos\beta} \\ & + \frac{8}{(5 + 2\sqrt{2}\cos\beta)^2} \theta_{12}^\ell \left(2\cos(\delta^\ell - \beta) + 2\sqrt{2}\cos\delta^\ell + \cos(\delta^\ell + \beta) \right) - \\ & - \frac{4}{(5 + 2\sqrt{2}\cos\beta)^2} \theta_{23}^\nu \left(4\cos\gamma + 2\sqrt{2}\cos(\gamma - \beta) + \sqrt{2}\cos(\beta + \gamma) \right) - \\ & - \frac{2}{5 + 2\sqrt{2}\cos\beta} \theta_{12}^\nu \left(2\cos\chi + \sqrt{2}\cos(\chi - \beta) \right) + \mathcal{O}(\theta_k^2) \end{aligned} \quad (22)$$

To *zeroth* order, $\sin^2\theta_{12} = 2/(5 + 2\sqrt{2}\cos\beta) = \sin^2\theta_{23}$. Together with the $\cos\beta \gtrsim 0.95$ constraint to *zeroth* order, this implies that $\sin^2\theta_{12} \simeq 2/(5 + 2\sqrt{2}) \simeq 0.26$ coincides very well with its current best-fit value.

For the sake of simplicity, we just show the *zeroth* order contribution for $\sin\delta_{\text{CP}}$ and $\cos\delta_{\text{CP}}$:

$$\sin\delta_{\text{CP}} = -\frac{(5 + 2\sqrt{2}\cos\beta)\sin\beta}{\sqrt{(-3 - 2\sqrt{2}\cos\beta)(-5 + 4\cos 2\beta)}} + \mathcal{O}(\theta_k) \quad (23)$$

$$\cos\delta_{\text{CP}} = \frac{\sqrt{2}\cos\beta + 2\cos 2\beta}{\sqrt{6 - 4\sqrt{2}\cos\beta(3 + 2\sqrt{2}\cos\beta)}} + \mathcal{O}(\theta_k). \quad (24)$$

Because $\cos\beta$ has to be large (and $|\beta|$ therefore has to be small), $|\sin\delta_{\text{CP}}|$ is small and $\cos\delta_{\text{CP}}$ is positive, *i.e.*, δ_{CP} is close to zero. Furthermore, $\sin\delta_{\text{CP}}$ has always the opposite

sign of $\sin\beta$. To *zeroth* order in the small mixing angles, $|\delta_{\text{CP}}| \lesssim \pi/3$, which means that maximal CP violation requires higher order corrections.

In summary, configuration 1 is characterized by large $\sin^2\theta_{13}$, strong deviations from maximal atmospheric mixing into the first octant, $\sin^2\theta_{12}$ close to its current best-fit value, and δ_{CP} close to 0. Therefore, future improved bounds on $\sin^2\theta_{13}$ and an improved precision for $\sin^2\theta_{23}$ can easily test this configuration. Note that this configuration does not look compatible with the tri-bimaximal mixing idea since $\sin^2\theta_{13}$ is intrinsically large and $\sin^2\theta_{23}$ strongly deviates from maximal mixing. Our procedure has been particularly simple in this case: We have expanded the observables in the small mixing angles, and we have discussed the implications of the current bounds on the unphysical quantities and observables. For example, we have found from the $\sin^2\theta_{13}$ bound that $\cos\beta = \cos(\delta^\ell - \delta^\nu - \phi_2)$ has to be close to one, and we have used this knowledge for the other observables. The next example will be more sophisticated in the sense that there are more qualitative cases.

3.2 Two maximal mixing angles: $(\theta_{12}^\ell, \theta_{13}^\ell, \theta_{23}^\ell, \theta_{12}^\nu, \theta_{13}^\nu, \theta_{23}^\nu) = (*, *, \frac{\pi}{4}, \frac{\pi}{4}, *, *)$

This configuration 2 is characterized by one large mixing in each the neutrino and charged lepton sectors, namely θ_{23}^ℓ and θ_{12}^ν . The small mixing angles θ_{12}^ℓ , θ_{13}^ℓ , θ_{13}^ν and θ_{23}^ν are, except from $\sin^2\theta_{13}$, expanded up to second order. Since there is one more small mixing angle than before, there is naturally more freedom involved in this case.

Again, we start the discussion of the observables with $\sin^2\theta_{13}$, which we expand to third order as⁵

$$\begin{aligned} \sin^2\theta_{13} = & \frac{1}{2} \theta_{12}^{\ell\,2} + \frac{1}{2} \theta_{13}^{\ell\,2} + \theta_{13}^{\nu\,2} - \cos\delta^\ell \theta_{12}^\ell \theta_{13}^\ell + \sqrt{2} \cos(\varphi_2 + \delta^\nu) \theta_{12}^\ell \theta_{13}^\nu \\ & - \sqrt{2} \cos(\varphi_2 - \delta^\ell + \delta^\nu) \theta_{13}^\ell \theta_{13}^\nu - 6 \cos(\varphi_1 - \varphi_2) \theta_{12}^{\ell\,2} \theta_{23}^\nu \\ & - 12 \sin\delta^\ell \sin(\varphi_1 - \varphi_2) \theta_{12}^\ell \theta_{13}^\ell \theta_{23}^\nu + 6 \cos(\varphi_1 - \varphi_2) \theta_{13}^{\ell\,2} \theta_{23}^\nu \\ & - 6\sqrt{2} \cos(\delta^\nu + \varphi_1) \theta_{12}^\ell \theta_{13}^\nu \theta_{23}^\nu - 6\sqrt{2} \cos(\delta^\nu + \varphi_1 - \delta^\ell) \theta_{13}^\ell \theta_{13}^\nu \theta_{23}^\nu + \mathcal{O}(\theta_k^4). \end{aligned} \quad (25)$$

Since $\sin^2\theta_{13}$ is zero to *zeroth* and first order, it is intrinsically small compared to that of configuration 1. However, if the small angles are chosen comparatively large, it is possible to generate a $\sin^2\theta_{13}$ close to the current bound. There is already one important qualitative difference observable at this place, which is different from configuration 1: If all small mixing angles are zero, δ_{CP} is not defined. This means that we will need to distinguish different cases determined by the non-vanishing small mixing angles.

The solar mixing angle is given by

$$\begin{aligned} \sin^2\theta_{12} = & \frac{1}{2} - \frac{1}{\sqrt{2}} \cos(\delta^\ell - \varphi_1) \theta_{13}^\ell - \frac{1}{\sqrt{2}} \cos\varphi_1 \theta_{12}^\ell \\ & - \frac{1}{\sqrt{2}} \cos\varphi_2 \theta_{12}^\ell \theta_{23}^\nu + \frac{1}{\sqrt{2}} \cos(\delta^\ell - \varphi_2) \theta_{13}^\ell \theta_{23}^\nu + \mathcal{O}(\theta_k^3), \end{aligned} \quad (26)$$

⁵We expand $\sin^2\theta_{13}$ to the third order in the small mixing angles because the leading contributions come from the second order terms, and the coefficients of the third order terms are comparatively large.

which is maximal to zeroth order. Therefore, in order to satisfy the bounds on $\sin^2 \theta_{12}$ in Eq. (18), at least one of the two small charged lepton angles θ_{12}^ℓ or θ_{13}^ℓ has to be moderately large. Nevertheless, $\sin^2 \theta_{12}$ close to its best-fit value will require some tuning of the phases. Note that once θ_{12}^ℓ or θ_{13}^ℓ is non-vanishing, an exactly vanishing $\sin^2 \theta_{13}$ in Eq. (25) will also require some tuning.

We expand $\sin^2 \theta_{23}$ to second order in the small angles:

$$\begin{aligned} \sin^2 \theta_{23} = & \frac{1}{2} - \cos(\varphi_1 - \varphi_2) \theta_{23}^\nu - \frac{1}{4} \theta_{12}^{\ell 2} + \frac{1}{4} \theta_{13}^{\ell 2} + \frac{1}{2} \cos \delta^\ell \theta_{13}^\ell \theta_{12}^\ell \\ & - \frac{1}{\sqrt{2}} \cos(\delta^\ell - \delta^\nu - \varphi_2) \theta_{13}^\ell \theta_{13}^\nu - \frac{1}{\sqrt{2}} \cos(\delta^\nu + \varphi_2) \theta_{12}^\ell \theta_{13}^\nu + \mathcal{O}(\theta_k^3). \end{aligned} \quad (27)$$

Obviously, $\sin^2 \theta_{23}$ is to zeroth order given by its best-fit value maximal mixing, and $\sin^2 \theta_{12}$ and $\sin^2 \theta_{23}$ are identical to zeroth order. Therefore, we do not obtain additional constraints from Eq. (18). However, we will see that the higher order contributions lead to interesting observations for deviations from maximal mixing and the θ_{23} octant.

As indicated above, we cannot calculate δ_{CP} as a expansion in the small angles without further assumptions. If all of the contributing small angles are zero, $\sin^2 \theta_{13}$ will be zero, and hence δ_{CP} will not be defined. In addition, at least one of the two angles θ_{12}^ℓ and θ_{13}^ℓ has to be sufficiently large to move $\sin^2 \theta_{12}$ in the currently allowed range. Therefore, we choose three different sets of small angles: all small angles zero except θ_{12}^ℓ , all small angles zero except θ_{13}^ℓ , and $\theta_{12}^\ell = \theta_{13}^\ell = \sqrt{\theta_{23}^\nu}$ with $\theta_{13}^\nu = 0$. The third case will allow us to construct tri-bimaximal mixing. In the following, we expand the observable mixing angles to second order and the observable Dirac CP phase to first order.

3.2.1 Non-vanishing θ_{12}^ℓ , and $\theta_{13}^\ell = \theta_{13}^\nu = \theta_{23}^\nu = 0$

In this case, we have

$$\sin^2 \theta_{13} = \frac{1}{2} (\theta_{12}^\ell)^2, \quad (28)$$

$$\sin^2 \theta_{12} = \frac{1}{2} - \frac{1}{\sqrt{2}} \cos \varphi_1 \theta_{12}^\ell, \quad (29)$$

$$\sin^2 \theta_{23} = \frac{1}{2} - \frac{1}{4} (\theta_{12}^\ell)^2, \quad (30)$$

$$\sin \delta_{\text{CP}} = \sin \varphi_1, \quad \cos \delta_{\text{CP}} = -\cos \varphi_1. \quad (31)$$

In Eq. (29), we have to choose the product $\cos \varphi_1 \theta_{12}^\ell$ positive and moderately large in order to be within the allowed range for $\sin^2 \theta_{12}$. This implies a significant deviation of $\sin^2 \theta_{13}$ from zero, and of $\sin^2 \theta_{23}$ from maximal mixing. Note that δ_{CP} is given by $\delta_{\text{CP}} = \pi - \varphi_1$, and that $\cos \varphi_1$ is constrained by the bound on $\sin^2 \theta_{12}$ (*cf.*, Eq. (18)) by $\cos \varphi_1 \gtrsim \sqrt{2}/(10 \theta_{12}^\ell)$. Therefore, δ_{CP} tends to be close to π , and maximal CP violation is forbidden because of $\cos \varphi_1 > 0$. Similarly, from $\theta_{12}^\ell \gtrsim \sqrt{2}/(10 \cos \varphi_1) \geq \sqrt{2}/10$, we obtain a lower bound $\sin^2 \theta_{13} \gtrsim 0.01$. This bound lies within the range of upcoming reactor experiments, such as Double Chooz (see, *e.g.*, Refs. [39, 40]).

As the next step, we can eliminate θ_{12}^ℓ in order to establish relationships among the physical observables. Such relationships are **type I sum rules** according to our definition:

$$\theta_{23} + \frac{1}{2} \theta_{13}^2 \simeq \frac{\pi}{4}, \quad (32)$$

$$\theta_{12} - \cos \delta_{\text{CP}} \theta_{13} \simeq \frac{\pi}{4}. \quad (33)$$

The deviation from maximal mixing described by Eq. (32), which can be as large as 3% from the $\sin^2 \theta_{13}$ upper bound in Eq. (18), is on the edge of future experiments (see, *e.g.*, Ref. [41]). In Eq. (33), the observables θ_{12} , θ_{13} , and δ_{CP} are related. Obviously, this case will be challenged for either better θ_{13} bounds, or a detection of $\theta_{13} > 0$ together with $\cos \delta_{\text{CP}} > 0$.

3.2.2 Non-vanishing θ_{13}^ℓ , and $\theta_{12}^\ell = \theta_{13}^\nu = \theta_{23}^\nu = 0$

Here we find

$$\sin^2 \theta_{13} = \frac{1}{2} (\theta_{13}^\ell)^2, \quad (34)$$

$$\sin^2 \theta_{12} = \frac{1}{2} - \frac{1}{\sqrt{2}} \cos(\delta^\ell - \varphi_1) \theta_{13}^\ell, \quad (35)$$

$$\sin^2 \theta_{23} = \frac{1}{2} + \frac{1}{4} (\theta_{13}^\ell)^2, \quad (36)$$

$$\sin \delta_{\text{CP}} = \sin(\delta^\ell - \varphi_1), \quad \cos \delta_{\text{CP}} = \cos(\delta^\ell - \varphi_1). \quad (37)$$

Obviously, we recover the same structure as in the previous case with $\theta_{13}^\ell \leftrightarrow \theta_{12}^\ell$ and $\delta^\ell - \varphi_1 \leftrightarrow \varphi_1$. The main differences can be easily seen in the type I sum rules

$$\theta_{23} - \frac{1}{2} \theta_{13}^2 \simeq \frac{\pi}{4}, \quad (38)$$

$$\theta_{12} + \cos \delta_{\text{CP}} \theta_{13} \simeq \frac{\pi}{4}. \quad (39)$$

Compared to Eq. (32), θ_{23} is now in the second octant, *i.e.*, the deviation from maximal mixing is positive instead of negative. The difference between these two cases should now be measurable by future experiments, because it is twice as big as the deviation from maximal mixing. In addition, this comparison motivates a precision octant measurement, which could discriminate which of θ_{12}^ℓ and θ_{13}^ℓ dominates in this framework. Compared to Eq. (33), δ_{CP} is now located at around 0 instead of π . This means that even if no CP violation is found in future experiments, it is interesting to distinguish these CP-conserving values (see, *e.g.*, Ref. [42] for precision measurements of δ_{CP}).

3.2.3 Large CP violation or tri-bimaximal mixing

Here we discuss the case $X \equiv \theta_{12}^\ell = \theta_{13}^\ell = \sqrt{\theta_{23}^\nu}$ and $\theta_{13}^\nu = 0$, *i.e.*, $(\theta_{12}^\ell, \theta_{13}^\ell, \theta_{23}^\ell, \theta_{12}^\nu, \theta_{13}^\nu, \theta_{23}^\nu) = (X, X, \frac{\pi}{4}, \frac{\pi}{4}, 0, X^2)$, in order to construct maximal CP violation or the tri-bimaximal case.

Observable	Mixing angle case $(\theta_{12}^\ell, \theta_{13}^\ell, \theta_{23}^\ell, \theta_{12}^\nu, \theta_{13}^\nu, \theta_{23}^\nu)$		
	$(Y, 0, \frac{\pi}{4}, \frac{\pi}{4}, 0, 0)$	$(0, Y, \frac{\pi}{4}, \frac{\pi}{4}, 0, 0)$	$(X, X, \frac{\pi}{4}, \frac{\pi}{4}, 0, X^2)$
θ_{12}	$\simeq \pi/4 + \cos \delta_{\text{CP}} \theta_{13}$	$\simeq \pi/4 - \cos \delta_{\text{CP}} \theta_{13}$	Any in currently allowed range
θ_{23}	$\simeq \pi/4 - \theta_{13}^2/2$	$\simeq \pi/4 + \theta_{13}^2/2$	Around maximal mixing
θ_{13}	$\gtrsim 0.1$	$\gtrsim 0.1$	Any in currently allowed range
δ_{CP}	$\sim \pi$	~ 0	$ \sin \delta_{\text{CP}} \gtrsim 0.4$ (if $\theta_{13} > 0$)

Table 1: Type I sum rules or approximative values/ranges for the observables δ_{CP} , θ_{13} , θ_{23} and θ_{12} for the three cases of configuration 2 (*cf.*, Secs. 3.2.1, 3.2.1, and 3.2.3). The angle Y refers to a mixing angle in the range $\sqrt{2}/10 \lesssim Y \lesssim \theta_C$, whereas the angle X lies within the range $\sqrt{2}/20 \lesssim X \lesssim \theta_C$. The conditions for the last column are much weaker than in the other two cases, because the dependence on three unphysical phases allows for more freedom.

For the observables, we find

$$\sin^2 \theta_{13} = X^2 (1 - \cos \delta^\ell) , \quad (40)$$

$$\sin^2 \theta_{12} = \frac{1}{2} - \frac{1}{\sqrt{2}} X (\cos(\delta^\ell - \varphi_1) + \cos \varphi_1) , \quad (41)$$

$$\sin^2 \theta_{23} = \frac{1}{2} (1 + (\cos \delta^\ell + 2 \cos(\varphi_1 - \varphi_2)) X^2) , \quad (42)$$

$$\sin \delta_{\text{CP}} = \frac{\sin(\delta^\ell - \varphi_1) + \sin \varphi_1}{\sqrt{2} - 2 \cos \delta^\ell} , \quad \cos \delta_{\text{CP}} = \frac{\cos(\delta^\ell - \varphi_1) - \cos \varphi_1}{\sqrt{2} - 2 \cos \delta^\ell} . \quad (43)$$

In comparison to the previous cases, we can have a vanishing $\sin^2 \theta_{13}$ here. Furthermore, $\sin^2 \theta_{13}$ and $\sin^2 \theta_{23}$ depend on the phase δ^ℓ . Except from that, the structure of the equations is similar to those of Secs. 3.2.1 and 3.2.2. For X , we obtain from Eqs. (18) and (41) the constraint $X \gtrsim \sqrt{2}/20 \simeq 0.07$.

Let us now focus on the possibility of maximal CP violation, which was excluded in the previous cases. For maximal CP violation, $\cos \delta_{\text{CP}} = 0$, and we obtain from Eq. (43) $\tan \varphi_1 = (1 - \cos \delta^\ell) / \sin \delta^\ell$. Using this condition in Eq. (40) and Eq. (41), one can show that $\sin^2 \theta_{12}$ and $\sin^2 \theta_{13}$ are compatible with their currently allowed ranges. For CP conservation, however, we obtain from $\sin \delta_{\text{CP}} = 0$ in Eq. (43) the condition $\tan \varphi_1 = \sin \delta^\ell / (\cos \delta^\ell - 1)$, which is incompatible with the $\sin^2 \theta_{12}$ allowed range. Therefore, CP conservation is excluded, and maximal CP violation is possible. More specifically, one can show that $|\sin \delta_{\text{CP}}| \gtrsim 0.4$ for $X \leq \theta_C$, *i.e.*, $|\delta_{\text{CP}}| \gtrsim \pi/8$ for $\cos \delta_{\text{CP}} > 0$. This implies that a future experiment will find the CP violation if the fraction of δ_{CP} , for which CP violation can be discovered, is about 75%. A neutrino factory would find such a CP violation for $\sin^2 2\theta_{13} \gtrsim 10^{-4}$ (see, *e.g.*, Fig. 23 in Ref. [43]).

We can construct tri-bimaximal mixing with this set of assumptions. For exactly tri-bimaximal mixing, the following equations have to be fulfilled: $\sin^2 \theta_{12} = 1/3$, $\sin^2 \theta_{13} = 0$, and $\sin^2 \theta_{23} = 1/2$. From Eq. (40), we first of all obtain $\delta^\ell = 0$. Therefore, Eqs. (41)

and (42) simplify to

$$\sin^2 \theta_{12} = \frac{1}{2} - \sqrt{2} \cos \varphi_1 X \stackrel{!}{=} \frac{1}{3} \quad (44)$$

$$\sin^2 \theta_{23} = \frac{1}{2} + X^2 \left(\frac{1}{2} - \cos(\varphi_1 - \varphi_2) \right) \stackrel{!}{=} \frac{1}{2}. \quad (45)$$

Eliminating φ_1 , the condition for tri-bimaximal mixing is then given in terms of φ_2 and X as

$$\cos\left(\frac{\pi}{3} \pm \varphi_2\right) X = \frac{1}{6\sqrt{2}}. \quad (46)$$

This condition can be fulfilled, for instance, for $\varphi_2 = \pi/3$ and $X = 1/(6\sqrt{2})$. This means that tri-bimaximal mixing can be constructed within configuration 2. Note that we have only expanded the small mixing angles to second order, which means that higher order corrections will act as small deviations from tri-bimaximal mixing. In addition, note that δ_{CP} is, of course, not defined if $\sin^2 \theta_{13}$ is exactly zero.

We summarize the three special cases discussed for configuration 2 in Table 1. These three cases can be easily distinguished: If $\sin^2 \theta_{13}$ is much smaller than 0.01, we have the third case. If $\sin^2 \theta_{13}$ is large, we can use δ_{CP} to disentangle all three cases. In addition, the θ_{23} octant could be used to discriminate between the first and second case.

4 Introducing mass matrix structure

In the preceding section, we have not made any special assumptions for the small mixing angles in our configurations. In this section, we extend the preceding discussion by two additional aspects:

- We assume that the small mixings angles $\theta_{ij}^\nu, \theta_{ij}^\ell$ in our configurations, which we have denoted by stars, can only come from the set $\{\epsilon, \epsilon^2, 0\}$, where $\epsilon \simeq \theta_C$.
- We discuss our configurations together with specific mass textures of the form of Eq. (7) for M_ν^{Maj} . This means that we include the form of specific mass matrices in the discussion, and that the individual texture entries can only be

$$T_{ij} = \eta^{n_{ij}} = \epsilon^{n_{ij}} \exp(in_{ij}\Phi) \quad (47)$$

with $n_{ij} \in \{0, 1, 2, \dots\}$ and an arbitrary but fixed phase Φ .

The first aspect establishes, similar to EQLC, a phenomenological connection to the quark sector. Therefore, we will obtain sum rules including the Cabibbo angle. The second aspect will constrain the physical observables and, especially, the Dirac and Majorana phases. In many cases, we will derive a relationship to the phase Φ . Of course, both of these aspects introduce more model-dependence than in the preceding section. However, we will also obtain stronger constraints from the textures.

#	$(\theta_{12}^\ell, \theta_{13}^\ell, \theta_{23}^\ell, \theta_{12}^\nu, \theta_{13}^\nu, \theta_{23}^\nu)$	T_ν^{Maj}	Φ	$(\theta_{12}^\ell, \theta_{13}^\ell, \theta_{23}^\ell, \delta^\ell, \theta_{12}^\nu, \theta_{13}^\nu, \theta_{23}^\nu, \delta^\nu, \varphi_1, \varphi_2, \alpha_1, \alpha_2)$ Obs.: $(s_{12}^2, s_{13}^2, s_{23}^2, \delta_{\text{CP}}, \phi_1, \phi_2)$
1a	$(*, \frac{\pi}{4}, \frac{\pi}{4}, *, \frac{\pi}{4}, *)$	$\begin{pmatrix} 1 & 0 & 1 \\ 0 & \eta & 0 \\ 1 & 0 & 1 \end{pmatrix}$	$\frac{\pi}{2}$	$(\epsilon^2, \frac{\pi}{4}, \frac{\pi}{4}, 0, 0, \frac{\pi}{4}, 0, 0, 0, 0, 0, 0.79)$ Obs.: $(0.29, 0.03, 0.25, 0, 0, 3.9)$
1b		$\begin{pmatrix} 1 & \eta & 1 \\ \eta & \eta & \eta \\ 1 & \eta & 1 \end{pmatrix}$	$\frac{\pi}{2}$	$(0, \frac{\pi}{4}, \frac{\pi}{4}, 0, \epsilon, \frac{\pi}{4}, \epsilon, 0, 1.57, 0, 0, 2.4)$ Obs.: $(0.30, 0.03, 0.26, 1.0, 5.9, 0.70)$
			$\frac{2\pi}{3}$	$(0, \frac{\pi}{4}, \frac{\pi}{4}, 0, \epsilon^2, \frac{\pi}{4}, \epsilon, 3.1, 5.2, 3.1, 0, 2.1)$ Obs.: $(0.29, 0.04, 0.31, 0.39, 3.1, 1.1)$
2a	$(*, *, \frac{\pi}{4}, \frac{\pi}{4}, *, *)$	$\begin{pmatrix} \eta & \eta & \eta^2 \\ \eta & \eta & 0 \\ \eta^2 & 0 & 1 \end{pmatrix}$	$\frac{\pi}{2}$	$(\epsilon, 0, \frac{\pi}{4}, 0, \frac{\pi}{4}, \epsilon^2, 0, 0, 0, 3.1, 0, 0.79)$ Obs.: $(0.36, 0.01, 0.50, 3.1, 0, 0.79)$
2b		$\begin{pmatrix} \eta & \eta & \eta \\ \eta & \eta & \eta^2 \\ \eta & \eta^2 & 1 \end{pmatrix}$	$\frac{\pi}{2}$	$(\epsilon, \epsilon, \frac{\pi}{4}, 4.7, \frac{\pi}{4}, \epsilon, 0, 1.6, 0, 3.1, 0, 0.79)$ Obs.: $(0.36, 0.02, 0.47, 2.8, 0.15, 0.65)$

Table 2: Possible textures for our two configurations if the small mixing angles (“*”) are chosen from the set $\{\epsilon, \epsilon^2, 0\}$ with $\epsilon = 0.2 \simeq \theta_C$. Note that one configuration may allow for different textures depending on the choices of the small mixing angles. The parameter $\eta = |\eta| \cdot \exp(i\Phi) = \epsilon \cdot \exp(i\Phi)$. The first column # refers to the texture number, the second to the configuration, and the third to the texture T_ν^{Maj} . The last two columns represent a possible implementation for each texture, *i.e.*, specific choices of Φ , the mixing angles and phases. This implementation includes the parameters used in Eq. (9) (first row), we well as the corresponding observables (second row, where $s_{ij} = \sin \theta_{ij}$). Note that texture (or angle) zeros correspond to $\mathcal{O}(\epsilon^3)$ in this table.

We list the textures which we will study in this section together with the corresponding configurations in Table 2. These textures have been found in Ref. [29] as valid patterns which can be fit to data by appropriate choices of the order one coefficients. We give in the last column one possible set of parameters corresponding to Eq. (11), which allows for a full construction of M_ν^{Maj} including order one coefficients for the Φ given in the second-last column (*cf.*, Sec. 2). In addition, for this set of parameters, the observables are given in the last column (second rows). The effective 3×3 Majorana texture is computed from Eq. (1) assuming a normal neutrino mass hierarchy of the form $m_1 : m_2 : m_3 = \epsilon^2 : \epsilon : 1$ (*cf.*, Eq. (6)). Note that for one configuration, there can be more possible textures, depending on the choices of the small mixing angles. Similarly, for one texture, there can be many valid sets of parameters, depending on the small mixing angles and phases used.

Our procedure for this section is as follows:

1. Given the textures in Table 2, we compute the additional constraints on the unphysical parameters. We require that the textures satisfy Eq. (47) and the small angles be only from the set $\{\epsilon, \epsilon^2, 0\}$. We list these additional constraints in Table 3, where the detailed procedure and a discussion of stability can be found in App. B.

Cond.	Texture 1a	Texture 1b	Texture 2a	Texture 2b
1	$\varphi_2 + \delta^\nu = 0$	$\varphi_2 + \delta^\nu = 0$	$\varphi_1 = 0$	$\varphi_1 = 0$
2	$2(\alpha_2 + \varphi_1 + \delta^\nu) = \Phi$	$2(\alpha_2 + \varphi_1 + \delta^\nu) = \Phi$	$2(\alpha_2 - \varphi_2) = \Phi$	$2(\alpha_2 - \varphi_2) = \Phi$
3	$\theta_{12}^\nu = \mathcal{O}(\epsilon^2)$	$\varphi_1 + \delta^\nu = \Phi$	$2\Phi = -\delta^\nu - \varphi_2$	$\Phi = -\delta^\nu - \varphi_2$
4	$\theta_{23}^\nu = \mathcal{O}(\epsilon^3)$	$\theta_{23}^\nu = \epsilon$	$\theta_{13}^\nu = \epsilon^2$	$\theta_{13}^\nu = \epsilon$
5			$\theta_{23}^\nu = \mathcal{O}(\epsilon^3)$	$\theta_{23}^\nu = \epsilon^2$ (for all Φ) or $\theta_{23}^\nu = \mathcal{O}(\epsilon^3)$ (for Φ in $\{\frac{\pi}{2}, \frac{3\pi}{2}\}$)

Table 3: Complete set of additional constraints obtained from the textures in Table 2. The first column refers to the condition number, the other columns to the different textures. For texture 2b and $\theta_{23}^\nu = \epsilon^2$, another non-trivial relationship $\varphi_2 = f(\Phi)$ can be derived, which can be simplified as $\varphi_2 \simeq -2\Phi$.

2. We apply the additional constraints in Table 3 to the analytical formulas obtained in Sec. 3. Now the observables depend on the configuration *and* texture, ϵ , and a number of unphysical parameters. Note that we only allow for possibilities within the current experimental bounds.
3. Neglecting higher order corrections, we use the analytical expressions to identify particularly simple relationships among the observables which satisfy our criteria for sum rules in Sec. 2.1. In addition, we identify the allowed regions as a function of the phases Φ and δ^ℓ for configuration 2, and we relate these phases to (observable) CP violation or conservation.

Note that one should regard the textures in Table 2 as the fundamental assumptions for this section, not the mixing angles from the above set, as it should be clear from App. B (see especially discussion in the very last paragraph).

For **textures 1a and 1b** from Table 2, we find that texture 1a is much more restrictive for the unphysical parameters than texture 1b (*cf.*, Table 3). For example, we obtain $(\sin^2 \theta_{23})_{1a} \simeq 2/(5 + 2\sqrt{2}) \simeq 0.26$ to zeroth order, which is somewhat below the currently allowed 3σ range. Therefore, the texture will be under tension even for the currently allowed θ_{23} range. In addition, we obtain a lower limit $\sin^2 \theta_{13} \gtrsim 0.02$ for texture 1a in comparison to Sec. 3.1, which is within the reach of upcoming reactor and superbeam experiments. For texture 1b, however, the observable mixing angles depend on the control parameter Φ . Since, for example, $\sin^2 \theta_{13}$ and $\sin^2 \theta_{23}$ strongly depend on Φ , it follows that not all possible Φ are allowed from the current bounds, *i.e.*, we need to approximately have Φ close to 2.6 or 3.7. For both textures 1a and 1b, we obtain **type IIIb sum rule** for the Majorana phase ϕ_2 as

$$(2\phi_2)_{1a, 1b} \simeq \Phi \quad (48)$$

to zeroth order, where maximal CP violation is obtained for $\Phi = \pi/2$ or $3\pi/2$. On the other hand, ϕ_1 will not be constrained in any of our examples. One can easily see that for the two textures here by re-writing Eq. (1) as

$$M_\nu^{\text{Maj}} = \text{diag}(1, e^{i\varphi_1}, e^{i\varphi_2}) \cdot \widehat{U}_\nu \cdot \text{diag}(\epsilon^2 e^{2i\alpha_1}, \epsilon e^{2i\alpha_2}, 1) \cdot \widehat{U}_\nu^T \cdot \text{diag}(1, e^{i\varphi_1}, e^{i\varphi_2}) . \quad (49)$$

	Texture 1a		Texture 1b	
Obs.	Sum rule/Range	(type)	Sum rule/Range	(type)
$\sin^2 \theta_{13}$	$\sin^2 \theta_{13} \in [0.02, 0.04]$		$\sin^2 \theta_{13} \simeq 0.04$	
$\sin^2 \theta_{12}$	$\sin^2 \theta_{12} \simeq 2/(5 + 2\sqrt{2})$	(I)	-	
	$\sin^2 \theta_{12} \simeq 0.26$		Any $\sin^2 \theta_{12}$ in allowed range	
$\sin^2 \theta_{23}$	$\sin^2 \theta_{23} \simeq 2/(5 + 2\sqrt{2})$	(I)	-	
	$\sin^2 \theta_{23} \simeq 0.26$		$\sin^2 \theta_{23} \in [0.34, 0.35]$	
δ_{CP}	$\delta_{\text{CP}} \simeq (1 - 3\sqrt{2})\delta^\ell$	(IIIa)	-	
	$\delta_{\text{CP}} \in [0, 0.6], [5.7, 2\pi)$		$\delta_{\text{CP}} \in [0, 0.8], [5.5, 2\pi)$	
$2\phi_2$	$2\phi_2 \simeq \Phi$	(IIIb)	$2\phi_2 \simeq \Phi$	(IIIb)
			$2\phi_2 \in [2.5, 2.7], [3.6, 3.8]$	

Table 4: Type I and III sum rules according to our classification for textures 1a and 1b, and approximate values/allowed ranges for the observables. The allowed ranges are obtained for $\epsilon = 0.2 \simeq \theta_C$, Φ varied within the allowed range, and all observables within their currently allowed 3σ ranges (except for texture 1a, where $\sin^2 \theta_{23}$ is slightly below this range). If no sum rule is given, we have not found one according to our definition.

Since α_1 always appears as a product with ϵ^2 for the normal hierarchy, and since the textures 1a and 1b do not have entries η^2 , we do not obtain a constraint on α_1 . From Eq. (9), we read off that α_1 adds to ϕ_1 , which means that ϕ_1 remains unconstrained. We summarize the allowed ranges (for any allowed Φ) and sum rules for textures 1a and 1b in Table 4.

For **textures 2a and 2b** from Table 2, we know from the discussion in Sec. 3.2 that $\sin^2 \theta_{13}$ is zero if all of the small mixing angles are chosen to be zero, which means that δ_{CP} can only be calculated for specific assumptions for the small mixing angles. In addition, $\sin^2 \theta_{12}$ tends to be too large (close to maximal) for this configuration. Therefore, we focus on $\sin^2 \theta_{12}$ first. We obtain for both textures

$$(\sin^2 \theta_{12})_{2a,2b} = \frac{1}{2} - \frac{1}{\sqrt{2}} \cos \delta^\ell \theta_{13}^\ell - \frac{1}{\sqrt{2}} \theta_{12}^\ell + \mathcal{O}(\epsilon^3). \quad (50)$$

We read off from this equation that at least one of the two angles θ_{12}^ℓ and θ_{13}^ℓ has to be of size ϵ , since otherwise $\sin^2 \theta_{12}$ violates its currently allowed range (*cf.*, Eq. (18)). The choices for θ_{12}^ℓ and θ_{13}^ℓ can only be $(\theta_{12}^\ell, \theta_{13}^\ell) \in \{(\epsilon, 0), (\epsilon, \epsilon^2), (0, \epsilon), (\epsilon^2, \epsilon), (\epsilon, \epsilon)\}$ from our allowed set of mixing angles. There are then only two small mixing angles remaining: θ_{13}^ν and θ_{23}^ν . For θ_{13}^ν , we now have $\theta_{13}^\nu = \epsilon^2$ (2a) or ϵ (2b) from Table 3. Therefore, we cannot use $\theta_{13}^\nu = 0$, as we have done in the special cases we have studied in Sec. 3.2. From Eq. (50), we already observe that not every value for δ_ℓ can be chosen if θ_{13}^ℓ is used to obtain a $\sin^2 \theta_{12}$ within the currently allowed range. As we find from the analytical expressions, Φ plays a similar role especially for $\sin^2 \theta_{13}$. Therefore, we obtain non-trivial constraints in the Φ - δ_ℓ plane from the currently allowed ranges, which will depend on the choices for θ_{12}^ℓ and θ_{13}^ℓ . We show these allowed regions in the Φ - δ_ℓ plane in Fig. 1 for texture 2a (left column) and texture 2b (right column) as shaded areas. The different rows correspond to the different

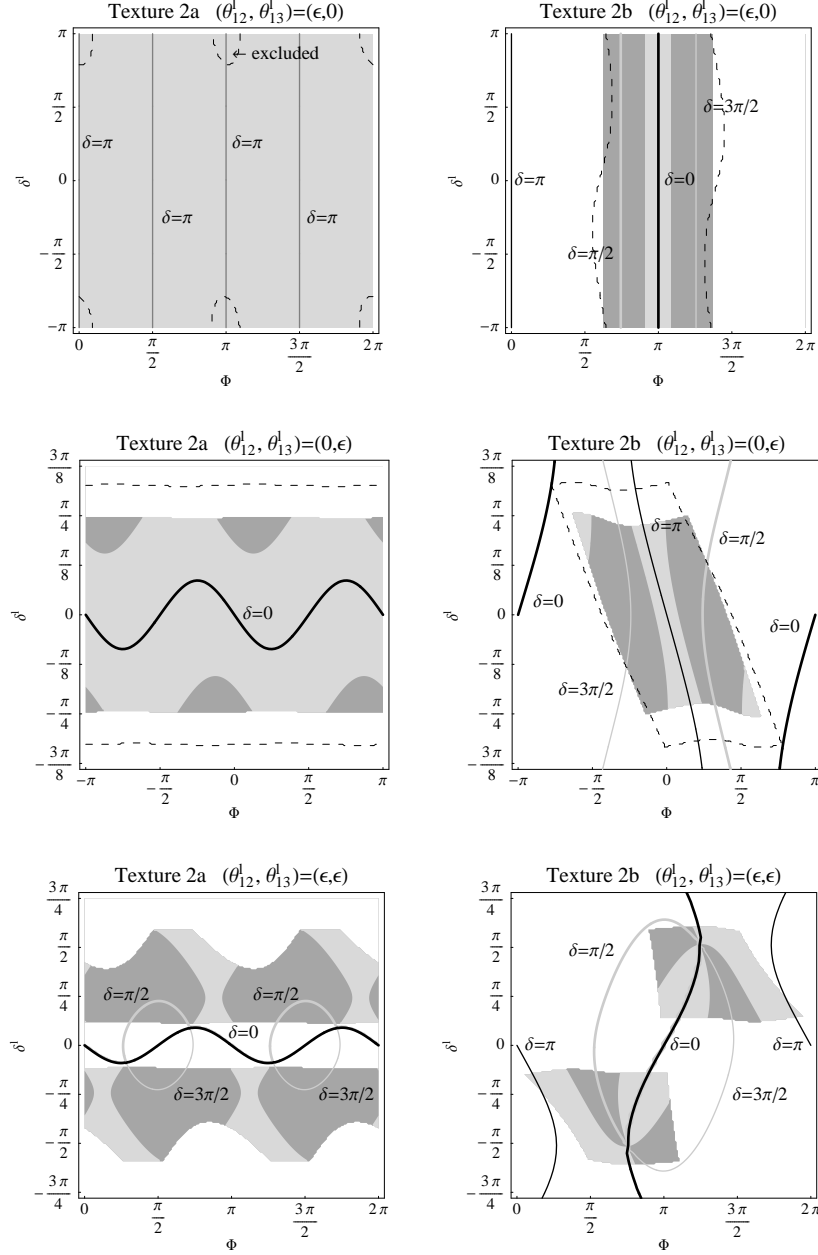


Figure 1: Allowed (shaded) regions in the Φ - δ_ℓ plane for texture 2a (left column) and texture 2b (right column) at the 3σ confidence level. The different rows correspond to the different $(\theta_{12}^\ell, \theta_{13}^\ell)$ cases, as given in the panel captions. In the first two rows, the corresponding allowed regions for the perturbed cases $(\theta_{12}^\ell, \theta_{13}^\ell) = (\epsilon, \epsilon^2)$ and (ϵ^2, ϵ) , respectively, are illustrated as dashed curves. In each panel, the solid curves mark four different cases for δ_{CP} : $\delta_{CP} = 0$ (thick black), $\delta_{CP} = \pi/2$ (thick gray), $\delta_{CP} = \pi$ (thin black), and $\delta_{CP} = 3\pi/2$ (thin gray), *i.e.*, gray curves correspond to maximal (Dirac) CP violation. In addition, the light (dark) shading within the regions refers to δ_{CP} closer to CP conservation (violation).

$(\theta_{12}^\ell, \theta_{13}^\ell)$ cases, as given in the panel captions. The dashed curves in the upper two rows represent the perturbed cases $(\theta_{12}^\ell, \theta_{13}^\ell) = (\epsilon, \epsilon^2)$ and (ϵ^2, ϵ) , respectively. Obviously, the deviations from the main cases $(\epsilon, 0)$ and $(0, \epsilon)$ are small. Therefore, we focus on the three cases $(\theta_{12}^\ell, \theta_{13}^\ell) \in \{(\epsilon, 0), (0, \epsilon), (\epsilon, \epsilon)\}$.

Following the procedure outlined above, we find a number of type II and III sum rules and restrictions for the allowed observable ranges for the different $(\theta_{12}^\ell, \theta_{13}^\ell)$ cases. We summarize our results in Table 5. As we have already mentioned in Sec. 2, the purpose of the sum rules can be very different, depending on the type. Here the type II sum rules can be used to falsify a model, whereas the type III sum rules can be used to actually measure an unphysical or model parameter within the respective model. From Table 5 we read off that, depending on the choices for the small mixings angles, either Φ or δ^ℓ can be reconstructed in many cases – such as from a measurement of θ_{12} or θ_{13} . Note that the allowed ranges in this table assume that any allowed value can be chosen for Φ . In a specific model, however, Φ can be a fixed parameter. If the observable is a function of Φ (and possibly other parameters), the allowed range will be constrained for a specific choice for Φ . In particular, we find that for both textures 2a and 2b, the parameters Φ and δ^ℓ control the value of δ_{CP} in all cases. We illustrate this dependence for the different cases in Fig. 1, where the different curves correspond to $\delta_{\text{CP}} = 0$ (thick black), $\delta_{\text{CP}} = \pi/2$ (thick gray), $\delta_{\text{CP}} = \pi$ (thin black), and $\delta_{\text{CP}} = 3\pi/2$ (thin gray), *i.e.*, gray curves correspond to maximal (Dirac) CP violation. In addition, the light (dark) shading within the regions refers to δ_{CP} closer to CP conservation (violation). In order to construct a model with (Dirac) CP violation, it turns out that texture 2a together with the choice $(\theta_{12}^\ell, \theta_{13}^\ell) = (\epsilon, \epsilon)$ (lower left panel) produces CP violation for any value of Φ . For specific values of Φ , texture 2b works in all cases of $(\theta_{12}^\ell, \theta_{13}^\ell)$ (right column). In these cases, the value of δ_{CP} will be mainly controlled by Φ , and the value of δ^ℓ is of secondary interest. The appearance of precisely the unphysical quantities Φ and δ^ℓ is not accidental. In Sec. 4, we have assumed that the Majorana neutrino mass matrix has a certain structure related to a model parameter Φ . However, we have not made any similar assumptions for the charged lepton mass matrix. Therefore, it is not surprising that one phase degree of freedom from each the neutrino and charged lepton sectors is remaining. The neutrino sector unphysical phases are, however, strongly determined by Φ and the texture. If one used similar assumptions for the charged lepton sector, one might be able to constrain δ^ℓ as well.

5 Summary and conclusions

In this study, we have focused on three key aspects: Entangled maximal mixings in $U_{\text{PMNS}} = U_\ell^\dagger U_\nu$, *i.e.*, maximal mixing angles in *both* U_ℓ and U_ν , CP violation in complex mass matrices, and a connection to the quark sector. Large mixing angles in both U_ℓ and U_ν can be motivated by Froggatt-Nielsen-like models, in which they naturally appear in both the charged lepton and neutrino sectors. The discussion of complex mass matrices can be motivated by the construction of CP violating models, and the connection to the quark sector can be motivated by quark-lepton unification.

In the first part of the study, we have focused on the aspect of entangled maximal mixings,

Texture 2a			Texture 2b		
Obs.	Sum rule/Range	(type)	Sum rule/Range	(type)	
$(\theta_{12}^\ell, \theta_{13}^\ell) = (\epsilon, 0)$					
$\sin^2 \theta_{13}$	$\theta_{13}^2 \simeq \frac{1}{2} \theta_C^2 + \sqrt{2} \cos(2\Phi) \theta_C^3$ $\sin^2 \theta_{13} \in [0.01, 0.03]$	(IIIb)	$\theta_{13}^2 \simeq \theta_C^2 (\frac{3}{2} + \sqrt{2} \cos \Phi)$ $\sin^2 \theta_{13} \in [0.003, 0.04]$	(IIIb)	
$\sin^2 \theta_{12}$	$\theta_{12} + \frac{1}{\sqrt{2}} \theta_C \simeq \frac{\pi}{4}$ $\sin^2 \theta_{12} \simeq 0.36$	(II)	$\theta_{12} + \frac{1}{\sqrt{2}} \theta_C \simeq \frac{\pi}{4}$ $\sin^2 \theta_{12} \simeq 0.36$	(II)	
$\sin^2 \theta_{23}$	$\theta_{23} + \frac{1}{4} \theta_C^2 \simeq \frac{\pi}{4}$ $\sin^2 \theta_{23} \simeq 0.49$	(II)	- $\sin^2 \theta_{23} \in [0.48, 0.51]$		
δ_{CP}	$\sin \delta_{\text{CP}} \simeq \sqrt{2} \theta_C \sin 2\Phi$ $\delta_{\text{CP}} \in [2.9, 3.4]$	(IIIb)	$\sin \delta_{\text{CP}} \simeq \frac{\sqrt{2} \sin \Phi}{\sqrt{3+2\sqrt{2} \cos \Phi}}$ $\delta_{\text{CP}} \in [0, 1.9], [4.4, 2\pi]$	(IIIb)	
$2\phi_2$	$2\phi_2 \simeq \Phi$ No restriction	(IIIb)	$2\phi_2 \simeq \Phi$ $2\phi_2 \in [1.9, 4.4]$	(IIIb)	
$(\theta_{12}^\ell, \theta_{13}^\ell) = (0, \epsilon)$					
$\sin^2 \theta_{13}$	$\sin^2 \theta_{13} \in [0.01, 0.03]$		$\sin^2 \theta_{13} \in [0.003, 0.04]$		
$\sin^2 \theta_{12}$	$\theta_{12} + \frac{1}{\sqrt{2}} \cos \delta^\ell \theta_C \simeq \frac{\pi}{4}$ $\sin^2 \theta_{12} \in [0.36, 0.4]$	(IIIa)	$\theta_{12} + \frac{1}{\sqrt{2}} \cos \delta^\ell \theta_C \simeq \frac{\pi}{4}$ $\sin^2 \theta_{12} \in [0.36, 0.4]$	(IIIa)	
$\sin^2 \theta_{23}$	$\theta_{23} - \frac{1}{4} \theta_C^2 \simeq \frac{\pi}{4}$ $\sin^2 \theta_{23} \simeq 0.51$	(II)	- $\sin^2 \theta_{23} \in [0.44, 0.54]$		
δ_{CP}	$\delta_{\text{CP}} \in [-1.1, 1.1]$		$\delta_{\text{CP}} \in [0.4, 2\pi - 0.4]$		
$2\phi_2$	$2\phi_2 \simeq \Phi$ No restriction	(IIIb)	$2\phi_2 \simeq \Phi$ $2\phi_2 \in [-2.0, 2.0]$	(IIIb)	
$(\theta_{12}^\ell, \theta_{13}^\ell) = (\epsilon, \epsilon)$					
$\sin^2 \theta_{12}$	$\theta_{12} + \frac{1}{\sqrt{2}} \theta_C (1 + \cos \delta^\ell) \simeq \frac{\pi}{4}$	(IIIa)	$\theta_{12} + \frac{1}{\sqrt{2}} \theta_C (1 + \cos \delta^\ell) \simeq \frac{\pi}{4}$	(IIIa)	
$\sin^2 \theta_{23}$	$\theta_{23} - \frac{1}{2} \theta_C^2 \cos \delta^\ell \simeq \frac{\pi}{4}$ $\sin^2 \theta_{23} \in [0.49, 0.52]$	(IIIa)	- $\sin^2 \theta_{23} \in [0.43, 0.55]$		
δ_{CP}	$\delta_{\text{CP}} \in [0.9, 2.7], [3.6, 5.4]$		No restriction		
$2\phi_2$	$2\phi_2 \simeq \Phi$ No restriction	(IIIb)	$2\phi_2 \simeq \Phi$ $2\phi_2 \in [0.3, 6.0]$	(IIIb)	

Table 5: Type II and III sum rules according to our classification for textures 2a and 2b, and approximate values/allowed ranges for the observables. The allowed ranges are obtained for $\epsilon = 0.2 \simeq \theta_C$, Φ varied within the allowed range, and all observables within their currently allowed 3σ ranges. The corresponding allowed regions in the Φ - δ^ℓ plane can be found in Fig. 1. If no sum rule is given, we have not found one according to our definition.

and we have discussed two specific configurations with mixing angles in U_ℓ and U_ν which can be either maximal, such as from a symmetry, or small (referred to by stars):

Configuration 1 with three max. mixing angles $(\theta_{12}^\ell, \theta_{13}^\ell, \theta_{23}^\ell, \theta_{12}^\nu, \theta_{13}^\nu, \theta_{23}^\nu) = (*, \frac{\pi}{4}, \frac{\pi}{4}, *, \frac{\pi}{4}, *)$

Configuration 2 with two max. mixing angles $(\theta_{12}^\ell, \theta_{13}^\ell, \theta_{23}^\ell, \theta_{12}^\nu, \theta_{13}^\nu, \theta_{23}^\nu) = (*, *, \frac{\pi}{4}, \frac{\pi}{4}, *, *)$

We have not made any further specific assumptions for the small mixing angles, expect that they are as small as they can be used for expansions. We have then computed the observables using invariants, and we have discussed the constraints from their currently allowed ranges. We have demonstrated that configuration 1 clearly prefers $\sin^2 \theta_{23}$ off maximal mixing at the lower end of the currently allowed range, $\sin^2 \theta_{12}$ close to its best-fit value, $\sin^2 \theta_{13}$ large, and $\delta_{\text{CP}} \simeq 0$. Configuration 2, on the other hand, prefers small $\sin^2 \theta_{13}$, $\sin^2 \theta_{12}$ at the upper end of the currently allowed range, and $\sin^2 \theta_{23}$ close to maximal mixing. We have distinguished three different cases for configuration 2, which lead to different results for $\sin^2 \theta_{13}$, δ_{CP} , and $\sin^2 \theta_{23}$. For example, we have found that testing the θ_{23} octant and δ_{CP} quadrant sum rules

$$\theta_{23} \pm \frac{1}{2}\theta_{13}^2 \simeq \frac{\pi}{4}, \quad \theta_{12} \mp \cos \delta_{\text{CP}} \theta_{13} \simeq \frac{\pi}{4} \quad (51)$$

may reveal if θ_{12}^ℓ (upper signs) or θ_{13}^ℓ (lower signs) is dominating. In addition, we have demonstrated how the tri-bimaximal mixing case can be constructed using configuration 2, and how CP violation can be obtained for $\theta_{12}^\ell = \theta_{13}^\ell = (\theta_{23}^\nu)^2$. Our estimate for the required experimental performance to find CP violation in that case requires a CP fraction of 75%, *i.e.*, CP violation needs to be discovered for 75% of all (true) values of δ_{CP} . In addition, the different qualitative cases discussed for configuration 2 have clearly demonstrated that $\sin^2 2\theta_{13}$ alone is not sufficient as a performance indicator. If $\sin^2 \theta_{13} \gtrsim 0.01$ within the Double Chooz accessible range, δ_{CP} can separate all the different cases. If $\sin^2 \theta_{13} \lesssim 0.01$, two cases can be excluded. Similarly, a precision $\sin^2 \theta_{23}$ octant measurement has turned out to be a good indicator.

In the second part of the study, we have linked the aspects of entangled maximal mixings and CP violation in complex mass matrices. We have assumed a normal hierarchy and specific complex neutrino mass textures for the effective 3×3 case, which are of the form $T_{ij} = \eta^{n_{ij}}$. Here η is a complex number and n_{ij} are real integer numbers. In this case, a unique phase $\Phi = \arg \eta$ controls the CP violation coming from the neutrino sector. In a Froggatt-Nielsen-like mechanism, it might be introduced as the relative phase between the VEVs of two Standard Model singlet scalar flavons fields, if the order one coefficients are assumed to be real and one field dominates the neutrino mass matrix. In that case, the n_{ij} 's are then solely determined by the quantum numbers of the fermions under a flavor symmetry. In order to establish a connection to the quark sector as well, we have, in the (extended) quark-lepton complementarity fashion, assumed that $|\eta| = \epsilon \simeq \theta_C$, *i.e.*, $\eta \simeq \theta_C \exp(i\Phi)$, and that all small angles can only be from the sequence $(\epsilon, \epsilon^2, \dots, 0)$. An example for such a complex texture can be found in Eq. (7).

We have demonstrated that the additional assumption of specific mass textures reduces the parameter space for the unphysical parameters significantly. In addition, a number of observables can be related to the model parameter Φ . For example, the Majorana phase

$2\phi_2$ (*cf.*, definition in Eq. (10)) has turned out to be approximately Φ in all cases to leading order, which means that maximal Majorana CP violation is obtained for $\Phi \in \{\pi/2, 3\pi/2\}$. For configuration 2, we have again distinguished different cases, where Φ and δ^ℓ have turned out to be the control parameters. We have demonstrated how to construct models with large CP violation, where, to a first approximation, Φ controls the specific value of δ_{CP} . However, in one case, CP conservation can be excluded for any Φ . We have summarized the allowed ranges in the Φ - δ^ℓ plane in Fig. 1, where one can also read off the values of δ_{CP} as a function of these control parameters. In addition, we have summarized all important relationships and observable constraints in Table 5.

As a very interesting feature of this study, a number of qualitatively different sum rules have emerged. Since the term “sum rule” is used in different contexts in the literature, we have defined it for our study, and we have classified the sum rules into three categories: Type I sum rules relate lepton sector (or quark sector) observables only. They can be used to falsify a model if all of the contributing observables (at least two) are measured (see, *e.g.*, Eq. (51)). Type II sum rules (QLC-type sum rules) relate at least one lepton sector observable with quark sector observables, such as the Cabibbo angle. They can be used to falsify a model if all of the contributing observables (at least one from the lepton sector) are measured (see, *e.g.*, Table 5). Type III sum rules relate lepton or quark sector observables with unphysical quantities (type IIIa), such as the phase δ^ℓ , or model parameters (type IIIb), such as the phase Φ . They can be used to obtain information on the unphysical quantities or model parameters with a specific model (see, *e.g.*, Table 5). In order to qualify as a sum rule, there can be only one such unphysical quantity according to our definition.

In conclusion, we have combined a number of aspects in this study: The concept of entangled maximal mixings, the concept of complex textures of the form $T_{ij} = \eta^{n_{ij}}$ as powers of a single complex number η , and the concept of quark-lepton complementarity for a connection to the quark sector. In addition, we have encountered a number of different classes of sum rules, which we have systematically studied. Our concepts have used specific configurations of maximal and small mixing angles, specific textures, and a normal neutrino mass hierarchy. However, they can be applied to different cases in the same way. In addition, note that we have considered the full complex case without any *a priori* assumptions on the unphysical phases. Finally, our concept of complex textures allows for a direct connection to discrete flavor symmetry models, such as in Ref. [30] on the one hand side, and for specific testable conclusions for future experiments on the other side. These conclusions are not only limited to performance indicators such as θ_{13} and deviations from maximal mixings, but are also applied to the Dirac and Majorana CP phases. For example, it has turned out that the value of δ_{CP} is a good performance indicator, even if no CP violation can be established.

Acknowledgments

WW would like to acknowledge support from Emmy Noether program of Deutsche Forschungsgemeinschaft.

A All possible found configurations

In Table 6, we list all possible configurations that we have found by choosing the mixing angles from the set $\{\pi/4, \epsilon, \epsilon^2, 0\}$ (for $\epsilon = 0.2$). In this table, we list the configuration, a possible implementation with a set of specific unphysical parameters in Eq. (11), and the corresponding physical observables. We require that the implementations pass the selection criterion

$$S \equiv \left(\frac{\sin^2 \theta_{12} - 0.3}{0.3 \times 0.09} \right)^2 + \left(\frac{\sin^2 \theta_{23} - 0.5}{0.5 \times 0.16} \right)^2 \leq 11.83, \quad \sin^2 \theta_{13} \leq 0.04. \quad (52)$$

This selector corresponds to compatibility at the 3σ confidence level (*cf.*, Eq. (18)) with a Gaussian χ^2 estimate for $\sin^2 \theta_{12}$ and $\sin^2 \theta_{23}$ (2 d.o.f.), and a hard cut for $\sin^2 \theta_{13}$. We do not show α_1 and α_2 , which can take any value because these phases simply add to the Majorana phases ϕ_1 and ϕ_2 for which we have not imposed any constraints yet. For the same reason, we do not show ϕ_1 and ϕ_2 . From the table, we can read off that we find a valid implementation for U_{PMNS} for 44 out of the theoretically possible $2^6 = 64$ configurations. Many of these configurations lead, however, to anarchic or semi-anarchic textures. The particular (subjective) choice of the two configurations in this paper is based on the following criteria:

- We have maximal mixings in both U_ℓ and U_ν
- We obtain interesting textures from the configuration, such as no anarchic patterns⁶
- We find solutions for the corresponding textures satisfying Eq. (47) for specific Φ
- We find solutions for M_ℓ as well satisfying these criteria (which is not a necessary condition, but might be required depending on the model)
- We find a strong impact of the condition Eq. (47) together with the corresponding textures on the allowed observable ranges

Therefore, we choose configurations #2 and #6 from this list for a more detailed analysis in this study.

B Additional constraints from textures

Here we clarify our definition of a texture, and we demonstrate how we derive the additional constraints coming from Eq. (47). First of all, we refer to the effective Majorana neutrino matrix entries as $(M_\nu^{\text{Maj}})_{ij}$, whereas the texture entries are referred to as T_{ij} . In order to obtain the texture entries, we expand

$$(M_\nu^{\text{Maj}})_{ij} = M_{ij}^{(0)} + M_{ij}^{(1)} \epsilon + M_{ij}^{(2)} \epsilon^2 + \mathcal{O}(\epsilon^3), \quad (53)$$

⁶Specifically, configurations with many maximal mixing angles tend to produce anarchic textures.

#	$(\theta_{12}^\ell, \theta_{13}^\ell, \theta_{23}^\ell, \theta_{12}^\nu, \theta_{13}^\nu, \theta_{23}^\nu)$	$(\theta_{12}^\ell, \theta_{13}^\ell, \theta_{23}^\ell, \delta^\ell, \theta_{12}^\nu, \theta_{13}^\nu, \theta_{23}^\nu, \delta^\nu, \varphi_1, \varphi_2)$	$(s_{12}^2, s_{13}^2, s_{23}^2, \delta_{\text{CP}})$
1	$(*, *, *, \frac{\pi}{4}, *, \frac{\pi}{4})$	$(\epsilon, \epsilon, \epsilon^2, 5.30, \frac{\pi}{4}, \epsilon, \frac{\pi}{4}, 4.71, 5.50, 1.37)$	$(0.30, 0.04, 0.50, 4.70)$
2	$(*, *, \frac{\pi}{4}, \frac{\pi}{4}, *, *)$	$(\epsilon, \epsilon, \frac{\pi}{4}, 0.59, \frac{\pi}{4}, \epsilon^2, \epsilon^2, 4.91, 5.89, 0.98)$	$(0.30, 0.01, 0.50, 2.56)$
3	$(\frac{\pi}{4}, *, \frac{\pi}{4}, *, \frac{\pi}{4}, *)$	$(\frac{\pi}{4}, \epsilon, \frac{\pi}{4}, 2.36, \epsilon^2, \frac{\pi}{4}, \epsilon, 0.79, 1.96, 2.16)$	$(0.30, 0.02, 0.50, 2.93)$
4	$(\frac{\pi}{4}, *, *, *, \frac{\pi}{4}, \frac{\pi}{4})$	$(\frac{\pi}{4}, \epsilon, \epsilon, 0.00, \epsilon^2, \frac{\pi}{4}, \frac{\pi}{4}, 2.75, 3.73, 4.12)$	$(0.30, 0.02, 0.50, 3.47)$
5	$(*, \frac{\pi}{4}, *, *, \frac{\pi}{4}, \frac{\pi}{4})$	$(\epsilon, \frac{\pi}{4}, \epsilon, 2.16, \epsilon^2, \frac{\pi}{4}, \frac{\pi}{4}, 5.11, 0.59, 3.93)$	$(0.30, 0.04, 0.43, 0.98)$
6	$(*, \frac{\pi}{4}, \frac{\pi}{4}, *, \frac{\pi}{4}, *)$	$(\epsilon, \frac{\pi}{4}, \frac{\pi}{4}, 1.96, \epsilon^2, \frac{\pi}{4}, \epsilon, 4.71, 0.79, 4.12)$	$(0.30, 0.04, 0.43, 0.95)$
7	$(*, *, \frac{\pi}{4}, \frac{\pi}{4}, *, \frac{\pi}{4})$	$(\epsilon, \epsilon, \frac{\pi}{4}, 0.98, \frac{\pi}{4}, \epsilon, \frac{\pi}{4}, 0.98, 6.09, 4.52)$	$(0.30, 0.01, 0.50, 2.87)$
8	$(\frac{\pi}{4}, \frac{\pi}{4}, *, *, \frac{\pi}{4}, \frac{\pi}{4})$	$(\frac{\pi}{4}, \frac{\pi}{4}, \epsilon, 0.00, \epsilon, \frac{\pi}{4}, \frac{\pi}{4}, 0.00, 0.39, 4.91)$	$(0.30, 0.00, 0.50, 2.61)$
9	$(\frac{\pi}{4}, \frac{\pi}{4}, \frac{\pi}{4}, *, \frac{\pi}{4}, *)$	$(\frac{\pi}{4}, \frac{\pi}{4}, \frac{\pi}{4}, 4.91, \epsilon, \frac{\pi}{4}, \epsilon^2, 0.20, 0.20, 3.53)$	$(0.30, 0.00, 0.50, 2.61)$
10	$(*, *, *, *, *, \frac{\pi}{4})$	$(\epsilon, \epsilon, \epsilon^2, 0.98, \epsilon, \epsilon, \frac{\pi}{4}, 0.59, 3.14, 0.98)$	$(0.22, 0.04, 0.49, 0.61)$
11	$(*, *, \frac{\pi}{4}, *, *, *)$	$(\epsilon, \epsilon, \frac{\pi}{4}, 0.00, \epsilon, \epsilon, \epsilon^2, 0.79, 3.14, 3.73)$	$(0.22, 0.04, 0.50, 4.49)$
12	$(\frac{\pi}{4}, *, *, \frac{\pi}{4}, \frac{\pi}{4}, \frac{\pi}{4})$	$(\frac{\pi}{4}, \epsilon, \epsilon, 0.79, \frac{\pi}{4}, \frac{\pi}{4}, \frac{\pi}{4}, 1.18, 4.91, 5.50)$	$(0.30, 0.04, 0.50, 0.46)$
13	$(\frac{\pi}{4}, *, \frac{\pi}{4}, \frac{\pi}{4}, \frac{\pi}{4}, *)$	$(\frac{\pi}{4}, \epsilon, \frac{\pi}{4}, 2.36, \frac{\pi}{4}, \frac{\pi}{4}, \epsilon, 1.57, 1.18, 1.37)$	$(0.30, 0.02, 0.50, 4.62)$
14	$(*, \frac{\pi}{4}, \frac{\pi}{4}, *, \frac{\pi}{4}, \frac{\pi}{4})$	$(\epsilon, \frac{\pi}{4}, \frac{\pi}{4}, 4.32, \epsilon^2, \frac{\pi}{4}, \frac{\pi}{4}, 1.57, 3.93, 1.57)$	$(0.30, 0.04, 0.50, 6.05)$
15	$(\frac{\pi}{4}, \frac{\pi}{4}, \frac{\pi}{4}, \frac{\pi}{4}, *, *)$	$(\frac{\pi}{4}, \frac{\pi}{4}, \frac{\pi}{4}, 0.39, \frac{\pi}{4}, \epsilon, \epsilon, 1.18, 5.30, 4.91)$	$(0.30, 0.02, 0.50, 3.88)$
16	$(\frac{\pi}{4}, \frac{\pi}{4}, *, \frac{\pi}{4}, *, \frac{\pi}{4})$	$(\frac{\pi}{4}, \frac{\pi}{4}, \epsilon, 2.95, \frac{\pi}{4}, \epsilon, \frac{\pi}{4}, 3.73, 5.30, 4.91)$	$(0.30, 0.02, 0.50, 3.89)$
17	$(\frac{\pi}{4}, *, \frac{\pi}{4}, *, \frac{\pi}{4}, \frac{\pi}{4})$	$(\frac{\pi}{4}, \epsilon, \frac{\pi}{4}, 2.16, \epsilon^2, \frac{\pi}{4}, \frac{\pi}{4}, 5.89, 1.37, 2.55)$	$(0.30, 0.02, 0.50, 3.11)$
18	$(*, \frac{\pi}{4}, *, \frac{\pi}{4}, \frac{\pi}{4}, \frac{\pi}{4})$	$(\epsilon, \frac{\pi}{4}, \epsilon, 4.12, \frac{\pi}{4}, \frac{\pi}{4}, \frac{\pi}{4}, 1.37, 5.50, 2.16)$	$(0.31, 0.04, 0.43, 0.67)$
19	$(*, \frac{\pi}{4}, \frac{\pi}{4}, \frac{\pi}{4}, \frac{\pi}{4}, *)$	$(\epsilon, \frac{\pi}{4}, \frac{\pi}{4}, 2.16, \frac{\pi}{4}, \frac{\pi}{4}, \epsilon, 4.71, 0.98, 4.32)$	$(0.29, 0.04, 0.43, 5.60)$
20	$(\frac{\pi}{4}, \frac{\pi}{4}, \frac{\pi}{4}, *, \frac{\pi}{4}, \frac{\pi}{4})$	$(\frac{\pi}{4}, \frac{\pi}{4}, \frac{\pi}{4}, 2.95, \epsilon, \frac{\pi}{4}, \frac{\pi}{4}, 4.32, 0.59, 5.11)$	$(0.30, 0.00, 0.50, 4.66)$
21	$(\frac{\pi}{4}, \frac{\pi}{4}, *, \frac{\pi}{4}, \frac{\pi}{4}, \frac{\pi}{4})$	$(\frac{\pi}{4}, \frac{\pi}{4}, \epsilon, 1.57, \frac{\pi}{4}, \frac{\pi}{4}, \frac{\pi}{4}, 3.93, 1.96, 4.91)$	$(0.30, 0.02, 0.50, 6.14)$
22	$(\frac{\pi}{4}, \frac{\pi}{4}, \frac{\pi}{4}, \frac{\pi}{4}, \frac{\pi}{4}, *)$	$(\frac{\pi}{4}, \frac{\pi}{4}, \frac{\pi}{4}, 5.11, \frac{\pi}{4}, \frac{\pi}{4}, \epsilon, 2.95, 0.59, 0.79)$	$(0.30, 0.02, 0.50, 5.28)$
23	$(\frac{\pi}{4}, \frac{\pi}{4}, \frac{\pi}{4}, \frac{\pi}{4}, *, \frac{\pi}{4})$	$(\frac{\pi}{4}, \frac{\pi}{4}, \frac{\pi}{4}, 2.16, \frac{\pi}{4}, \epsilon, \frac{\pi}{4}, 3.73, 5.89, 4.71)$	$(0.30, 0.03, 0.50, 3.37)$
24	$(*, \frac{\pi}{4}, *, *, *, \frac{\pi}{4})$	$(\epsilon, \frac{\pi}{4}, \epsilon^2, 4.91, \epsilon, \epsilon, \frac{\pi}{4}, 2.36, 0.79, 2.55)$	$(0.29, 0.04, 0.59, 3.50)$
25	$(*, \frac{\pi}{4}, \frac{\pi}{4}, *, *, *)$	$(\epsilon, \frac{\pi}{4}, \frac{\pi}{4}, 6.09, \epsilon, \epsilon, \epsilon^2, 5.30, 5.30, 0.79)$	$(0.30, 0.04, 0.59, 2.75)$
26	$(\frac{\pi}{4}, \frac{\pi}{4}, *, \frac{\pi}{4}, *, *)$	$(\frac{\pi}{4}, \frac{\pi}{4}, \epsilon, 5.89, \frac{\pi}{4}, \epsilon, \epsilon, 0.98, 0.98, 3.73)$	$(0.30, 0.03, 0.49, 4.73)$
27	$(\frac{\pi}{4}, *, \frac{\pi}{4}, *, *, \frac{\pi}{4})$	$(\frac{\pi}{4}, \epsilon, \frac{\pi}{4}, 4.52, \epsilon, \epsilon, \frac{\pi}{4}, 2.55, 4.71, 6.09)$	$(0.30, 0.04, 0.48, 6.05)$
28	$(*, *, \frac{\pi}{4}, *, *, \frac{\pi}{4})$	$(\epsilon, \epsilon, \frac{\pi}{4}, 1.57, \epsilon, \epsilon, \frac{\pi}{4}, 3.53, 3.93, 2.36)$	$(0.22, 0.04, 0.50, 5.12)$
29	$(\frac{\pi}{4}, *, *, *, *, \frac{\pi}{4})$	$(\frac{\pi}{4}, \epsilon, \epsilon, 2.16, \epsilon, \epsilon, \frac{\pi}{4}, 5.11, 0.98, 0.00)$	$(0.30, 0.03, 0.48, 0.29)$
30	$(\frac{\pi}{4}, *, *, *, *, *)$	$(\frac{\pi}{4}, \epsilon, \epsilon, 0.00, \epsilon, \epsilon, \epsilon, 0.00, 0.00, 3.14)$	$(0.30, 0.00, 0.29, 0.00)$
31	$(\frac{\pi}{4}, *, \frac{\pi}{4}, *, *, *)$	$(\frac{\pi}{4}, \epsilon, \frac{\pi}{4}, 0.39, \epsilon, \epsilon, \epsilon, 3.34, 0.98, 0.00)$	$(0.30, 0.03, 0.48, 0.27)$
32	$(\frac{\pi}{4}, *, \frac{\pi}{4}, \frac{\pi}{4}, \frac{\pi}{4}, \frac{\pi}{4})$	$(\frac{\pi}{4}, \epsilon, \frac{\pi}{4}, 5.69, \frac{\pi}{4}, \frac{\pi}{4}, \frac{\pi}{4}, 0.00, 5.69, 4.52)$	$(0.30, 0.03, 0.50, 2.27)$
33	$(\frac{\pi}{4}, \frac{\pi}{4}, \frac{\pi}{4}, \frac{\pi}{4}, \frac{\pi}{4}, \frac{\pi}{4})$	$(\frac{\pi}{4}, \frac{\pi}{4}, \frac{\pi}{4}, 3.14, \frac{\pi}{4}, \frac{\pi}{4}, \frac{\pi}{4}, 2.36, 2.75, 0.98)$	$(0.30, 0.01, 0.50, 5.89)$
34	$(*, \frac{\pi}{4}, \frac{\pi}{4}, \frac{\pi}{4}, \frac{\pi}{4}, \frac{\pi}{4})$	$(\epsilon, \frac{\pi}{4}, \frac{\pi}{4}, 5.11, \frac{\pi}{4}, \frac{\pi}{4}, \frac{\pi}{4}, 0.20, 5.89, 3.53)$	$(0.30, 0.03, 0.51, 1.53)$
35	$(*, \frac{\pi}{4}, *, \frac{\pi}{4}, *, \frac{\pi}{4})$	$(\epsilon, \frac{\pi}{4}, \epsilon^2, 1.37, \frac{\pi}{4}, \epsilon, \frac{\pi}{4}, 1.96, 1.18, 5.69)$	$(0.29, 0.04, 0.59, 4.76)$
36	$(*, \frac{\pi}{4}, \frac{\pi}{4}, \frac{\pi}{4}, *, *)$	$(\epsilon, \frac{\pi}{4}, \frac{\pi}{4}, 0.00, \frac{\pi}{4}, \epsilon, \epsilon^2, 2.95, 5.11, 3.34)$	$(0.30, 0.04, 0.59, 1.41)$
37	$(*, \frac{\pi}{4}, \frac{\pi}{4}, *, *, \frac{\pi}{4})$	$(\epsilon, \frac{\pi}{4}, \frac{\pi}{4}, 0.98, \epsilon, \epsilon, \frac{\pi}{4}, 0.79, 1.18, 5.69)$	$(0.29, 0.04, 0.65, 2.85)$
38	$(\frac{\pi}{4}, *, *, \frac{\pi}{4}, *, \frac{\pi}{4})$	$(\frac{\pi}{4}, \epsilon, \epsilon, 2.16, \frac{\pi}{4}, \epsilon, \frac{\pi}{4}, 0.98, 5.30, 4.32)$	$(0.30, 0.04, 0.48, 4.47)$
39	$(\frac{\pi}{4}, *, \frac{\pi}{4}, \frac{\pi}{4}, *, *)$	$(\frac{\pi}{4}, \epsilon, \frac{\pi}{4}, 0.39, \frac{\pi}{4}, \epsilon, \epsilon, 5.50, 5.30, 4.32)$	$(0.30, 0.04, 0.48, 4.44)$
40	$(\frac{\pi}{4}, *, *, \frac{\pi}{4}, *, *)$	$(\frac{\pi}{4}, \epsilon, \epsilon, 0.00, \frac{\pi}{4}, \epsilon, \epsilon, 1.18, 5.11, 1.96)$	$(0.31, 0.00, 0.29, 4.71)$
41	$(\frac{\pi}{4}, *, \frac{\pi}{4}, \frac{\pi}{4}, *, \frac{\pi}{4})$	$(\frac{\pi}{4}, \epsilon, \frac{\pi}{4}, 1.37, \frac{\pi}{4}, \epsilon, \frac{\pi}{4}, 3.53, 1.77, 0.39)$	$(0.29, 0.04, 0.49, 1.89)$
42	$(*, \frac{\pi}{4}, \frac{\pi}{4}, \frac{\pi}{4}, *, \frac{\pi}{4})$	$(\epsilon, \frac{\pi}{4}, \frac{\pi}{4}, 0.98, \frac{\pi}{4}, \epsilon, \frac{\pi}{4}, 0.20, 1.57, 6.09)$	$(0.30, 0.03, 0.65, 4.34)$
43	$(\frac{\pi}{4}, \frac{\pi}{4}, *, \frac{\pi}{4}, \frac{\pi}{4}, *)$	$(\frac{\pi}{4}, \frac{\pi}{4}, \epsilon, 0.98, \frac{\pi}{4}, \frac{\pi}{4}, \epsilon, 3.53, 1.57, 4.91)$	$(0.30, 0.04, 0.34, 3.77)$
44	$(\frac{\pi}{4}, \frac{\pi}{4}, *, *, \frac{\pi}{4}, *)$	$(\frac{\pi}{4}, \frac{\pi}{4}, \epsilon, 1.57, \epsilon, \frac{\pi}{4}, \epsilon, 4.91, 0.59, 3.93)$	$(0.31, 0.02, 0.27, 3.12)$

Table 6: All possible configurations (and implementation examples) found in the study. See main text for more explanations.

with $\epsilon \simeq \theta_C$ real, which means that the $M_{ij}^{(k)}$'s are complex numbers. Let the first non-vanishing coefficient for any i, j be $M_{ij}^{(n_{ij})}$, i.e., $|M_{ij}^{(n_{ij})}| > 0$ and $|M_{ij}^{(r)}| = 0$ for all $r < n_{ij}$. Then, if Eq. (47) holds, the leading order term can be written as

$$M_{ij}^{(n_{ij})} \epsilon^{n_{ij}} = e^{i\Pi} M K_{ij} \eta^{n_{ij}} = e^{i\Pi} M K_{ij} (\epsilon^{n_{ij}} e^{i\Phi n_{ij}}) \equiv e^{i\Pi} M K_{ij} T_{ij} \quad (54)$$

with $K_{ij} > 0$, real, and order unity, Π a global phase independent of i and j , and M the absolute neutrino mass scale. Therefore, the texture entry T_{ij} is defined as $T_{ij} \equiv \eta^{n_{ij}}$. The matrix is therefore determined by the texture entries T_{ij} except from a global phase (which can be absorbed in the field definitions), the absolute neutrino mass scale, real order one coefficients K_{ij} , and higher order corrections.⁷ If all $M_{ij}^{(k)} = 0$ for $0 \leq k \leq 2$, we use a texture “zero” with an undefined phase. This cutoff can be motivated by the current measurement precision, which does not allow for the discrimination of higher order terms. Consequently, we only choose values ϵ , ϵ^2 , and 0 for the small mixing angles, where the zero refers to mixing angles $\mathcal{O}(\epsilon^3)$.⁸

As the next step, let us illustrate how we obtain additional constraints from the textures. For a given configuration, we compute $(M_\nu^{\text{Maj}})_{ij}$ in Eq. (1) using $M_\nu^{\text{diag}} \propto (\epsilon^2, \epsilon, 1)$ and U_ν from the respective configuration. We apply Eq. (53) to $(M_\nu^{\text{Maj}})_{ij}$ and identify the leading order term. Then we obtain the texture entry T_{ij} from Eq. (54) by neglecting $M K_{ij}$ (we keep the global phase to explicitly eliminate one of the phases). We refer to this texture extraction mechanism as “ $(M_\nu^{\text{Maj}})_{ij} \rightarrow e^{i\Pi} T_{ij}$ ”. The texture entry T_{ij} has then to be matched to the corresponding texture in Table 2, which leads to additional constraints for the neutrino parameters. These constraints may in some cases depend on Φ . Note that not all of the neutrino parameters can be constrained by this procedure, and that the charged lepton parameters in U_ℓ remain untouched. One could extend this procedure to the charged lepton sector with corresponding textures, but this would be way more complicated because of the additional freedom coming from U'_ℓ in Eq. (2). In addition, in Froggatt-Nielsen-like models, a second field could be present in the charged lepton mass matrix in order to produce the stronger hierarchy.

Let us illustrate the texture extraction with several qualitatively different examples from configuration 1 (the examples hold for both textures 1a and 1b). First of all, we compute $(M_\nu^{\text{Maj}})_{ij}$ from Eq. (1), and expand it according to Eq. (53). For the 11-element, it is sufficient to expand to *zeroth* order as

$$(M_\nu^{\text{Maj}})_{11} = \frac{1}{2} e^{-2i\delta^\nu} + \mathcal{O}(\epsilon) \rightarrow e^{i\Pi} T_{11} = e^{i\Pi} 1, \quad (55)$$

where the “1” on the right is the 11-texture entry T_{11} from Table 2. Therefore, we can fix the global phase as $\Pi = -2\delta^\nu$, and we do not obtain any conditions for the angles. Similar

⁷Here the underlying assumption is that the complex phases in M_ν^{Maj} , and therefore the observables, are to leading order determined by $\eta^{n_{ij}}$ (cf., Eq. (3)). However, higher order corrections are used in Refs. [2,3,29] to fit the data, which means that they need to be absorbed in the leading order one coefficients K_{ij} . In the complex case, these higher order corrections can have complex coefficients, which means that the leading order K_{ij} 's are, in practice, not real but only “sufficiently real”. One can show that “sufficiently real” means that $|\arg(K_{ij})| \lesssim \theta_C \simeq 12^\circ$. Our conclusions for the phases will therefore only hold up to this precision.

⁸In some cases, we will use expansions up to the third order if there are no *zeroth* and first order terms. In this case, the contributions of the third order terms could be sizeable.

to that, we will always choose a texture entry $T_{ij} = 1$ to fix the global phase. We then expand the element $(M_\nu^{\text{Maj}})_{22}$ to first order as

$$(M_\nu^{\text{Maj}})_{22} = e^{2i(\alpha_2 + \varphi_1)} \epsilon + \mathcal{O}(\epsilon^2) \rightarrow e^{i\Pi} T_{22} = e^{i\Pi} \epsilon e^{i\Phi}. \quad (56)$$

Here the ϵ comes from the diagonal neutrino mass matrix M_ν^{diag} . Again, we obtain no condition for the angles, but only for the phases: $2(\alpha_2 + \varphi_1) = \Pi + \Phi$, or $2(\alpha_2 + \varphi_1 + \delta_\nu) = \Phi$. It relates a combination of unphysical phases to the model parameter Φ . The next element $(M_\nu^{\text{Maj}})_{12}$ is, to second order, given by

$$(M_\nu^{\text{Maj}})_{12} = \frac{1}{2} e^{i(\varphi_1 - \delta^\nu)} \theta_{23}^\nu + \frac{1}{\sqrt{2}} e^{i(2\alpha_2 + \varphi_1)} \theta_{12}^\nu \epsilon + \mathcal{O}(\epsilon^3) \rightarrow \begin{cases} T_{12} = 0 & (1a) \\ e^{i\Pi} T_{12} = e^{i\Pi} \eta & (1b) \end{cases} \quad (57)$$

This example nicely demonstrates the appearance of a mixed $\theta_{12}^\nu \epsilon$ -term, where the ϵ comes from the neutrino mass hierarchy $M_\nu^{\text{diag}} = (\epsilon^2, \epsilon, 1)$. Compared to the previous section, where we assumed the small mixing angles to be $\mathcal{O}(\epsilon)$ in order to expand in them, we now have a discrete set of possibilities $\theta_{ij}^\nu, \theta_{ij}^\ell \in \{\epsilon, \epsilon^2, 0\}$. In the expansion Eq. (53), however, the order of θ_{ij}^ν is not specified without additional assumptions. Therefore, the initial expansion will contain ϵ 's as well as θ_{ij}^ν 's. For texture 1a, T_{12} is zero, which means that all terms of the order lower than ϵ^3 have to vanish. Therefore, we have to choose $\theta_{23}^\nu = \mathcal{O}(\epsilon^3)$ and $\theta_{12}^\nu = \mathcal{O}(\epsilon^2)$ as that they only appear in combinations $\mathcal{O}(\epsilon^3)$. For texture 1b, T_{12} is η , which means that $(M_\nu^{\text{Maj}})_{12}$ must have a non-vanishing first order term. That can only come from $\theta_{23}^\nu = \epsilon$ because $\theta_{12}^\nu = \mathcal{O}(\epsilon)$. For the phases, we obtain in this case $\varphi_1 - \delta^\nu = \Pi + \Phi$, or $\varphi_1 + \delta^\nu = \Phi$.

We calculate the conditions on the angles and the phases for the other matrix elements and textures in the same way. The complete list of results are given in Table 3. Note that we do not use cancellations of terms to derive these constraints. For example, in Eq. (57), one may as well choose $\theta_{23}^\nu = \epsilon$, $\theta_{12}^\nu = \epsilon/\sqrt{2}$, and appropriate phases to cancel the two terms and have $T_{12} = 0$. In this case, θ_{12}^ν is not chosen from the set $\{\epsilon, \epsilon^2, 0\}$, but is only of the order ϵ . However, as a consequence, the conditions derived from this choice would not be stable under the variation of the angles by order one coefficients. For our choices, the angles and the mass hierarchy entries can be varied by order one coefficients, and therefore, our conditions are stable. Conversely, a variation of the order one coefficients in the textures does not change our conclusions as long as the phases of these variations are $\mathcal{O}(\theta_C)$. This aspect might be relevant for Froggatt-Nielsen-like models, where, in general, arbitrary order one coefficients are allowed. The stability criterion will hold until we use a specific $\epsilon = 0.2$ for numerical estimates, or we replace $\epsilon \rightarrow \theta_C$ to derive type II (or type III) sum rules.

References

- [1] P. H. Frampton, S. T. Petcov, and W. Rodejohann, Nucl. Phys. **B687**, 31 (2004), hep-ph/0401206.
- [2] F. Plentinger, G. Seidl, and W. Winter, Nucl. Phys. **B791**, 60 (2008), hep-ph/0612169.

- [3] F. Plentinger, G. Seidl, and W. Winter, Phys. Rev. **D76**, 113003 (2007), [arXiv:0707.2379\[hep-ph\]](#).
- [4] C. D. Froggatt and H. B. Nielsen, Nucl. Phys. **B147**, 277 (1979).
- [5] T. Enkhbat and G. Seidl, Nucl. Phys. **B730**, 223 (2005), [hep-ph/0504104](#).
- [6] G. Altarelli, F. Feruglio, and I. Masina, Nucl. Phys. **B689**, 157 (2004), [hep-ph/0402155](#).
- [7] A. Romanino, Phys. Rev. **D70**, 013003 (2004), [hep-ph/0402258](#).
- [8] S. Antusch and S. F. King, Phys. Lett. **B591**, 104 (2004), [hep-ph/0403053](#).
- [9] C. A. de S. Pires, J. Phys. **G30**, B29 (2004), [hep-ph/0404146](#).
- [10] N. Li and B.-Q. Ma, Eur. Phys. J. **C42**, 17 (2005), [hep-ph/0504161](#).
- [11] T. Ohlsson, Phys. Lett. **B622**, 159 (2005), [hep-ph/0506094](#).
- [12] K. A. Hochmuth, S. T. Petcov, and W. Rodejohann, Phys. Lett. **B654**, 177 (2007), [arXiv:0706.2975\[hep-ph\]](#).
- [13] I. Masina, Phys. Lett. **B633**, 134 (2006), [hep-ph/0508031](#).
- [14] S. T. Petcov and A. Y. Smirnov, Phys. Lett. **B322**, 109 (1994), [hep-ph/9311204](#).
- [15] A. Y. Smirnov (2004), [hep-ph/0402264](#).
- [16] M. Raidal, Phys. Rev. Lett. **93**, 161801 (2004), [hep-ph/0404046](#).
- [17] H. Minakata and A. Y. Smirnov, Phys. Rev. **D70**, 073009 (2004), [hep-ph/0405088](#).
- [18] M. Jezabek and Y. Sumino, Phys. Lett. **B457**, 139 (1999), [hep-ph/9904382](#).
- [19] C. Giunti and M. Tanimoto, Phys. Rev. **D66**, 113006 (2002), [hep-ph/0209169](#).
- [20] S. Antusch and S. F. King, Phys. Lett. **B631**, 42 (2005), [hep-ph/0508044](#).
- [21] S. K. Kang, C. S. Kim, and J. Lee, Phys. Lett. **B619**, 129 (2005), [hep-ph/0501029](#).
- [22] K. Cheung, S. K. Kang, C. S. Kim, and J. Lee, Phys. Rev. **D72**, 036003 (2005), [hep-ph/0503122](#).
- [23] B. C. Chauhan, M. Picariello, J. Pulido, and E. Torrente-Lujan, Eur. Phys. J. **C50**, 573 (2007), [hep-ph/0605032](#).
- [24] W. Rodejohann, Phys. Rev. **D69**, 033005 (2004), [hep-ph/0309249](#).
- [25] N. Li and B.-Q. Ma, Phys. Rev. **D71**, 097301 (2005), [hep-ph/0501226](#).
- [26] Z.-z. Xing, Phys. Lett. **B618**, 141 (2005), [hep-ph/0503200](#).

- [27] A. Datta, L. Everett, and P. Ramond, Phys. Lett. **B620**, 42 (2005), [hep-ph/0503222](#).
- [28] L. L. Everett, Phys. Rev. **D73**, 013011 (2006), [hep-ph/0510256](#).
- [29] W. Winter, Phys. Lett. **B659**, 275 (2008), [arXiv:0709.2163\[hep-ph\]](#).
- [30] F. Plentinger, G. Seidl, and W. Winter, JHEP **04**, 077 (2008), [0802.1718](#).
- [31] F. Plentinger and G. Seidl (2008), [arXiv:0803.2889\[hep-ph\]](#).
- [32] T. D. Lee, Phys. Rept. **9**, 143 (1974).
- [33] M. M. Robinson and J. Ziabicki (1997), [hep-ph/9705418](#).
- [34] S. Kanemura *et al.*, Eur. Phys. J. **C51**, 927 (2007), [arXiv:0704.0697\[hep-ph\]](#).
- [35] S. F. King, JHEP **08**, 105 (2005), [hep-ph/0506297](#).
- [36] E. Jenkins and A. V. Manohar, Nucl. Phys. **B792**, 187 (2008), [arXiv:0706.4313\[hep-ph\]](#).
- [37] C. Jarlskog, Phys. Rev. Lett. **55**, 1039 (1985).
- [38] T. Schwetz, Phys. Scripta **T127**, 1 (2006), [hep-ph/0606060](#).
- [39] P. Huber, J. Kopp, M. Lindner, M. Rolinec, and W. Winter, JHEP **05**, 072 (2006), [hep-ph/0601266](#).
- [40] F. Ardellier *et al.* (Double Chooz) (2006), [hep-ex/0606025](#).
- [41] S. Antusch, P. Huber, J. Kersten, T. Schwetz, and W. Winter, Phys. Rev. **D70**, 097302 (2004), [hep-ph/0404268](#).
- [42] P. Huber, M. Lindner, and W. Winter, JHEP **05**, 020 (2005), [hep-ph/0412199](#).
- [43] P. Huber, M. Lindner, M. Rolinec, and W. Winter, Phys. Rev. **D74**, 073003 (2006), [hep-ph/0606119](#).